

Three-Point Functions and $\mathfrak{su}(1|1)$ Spin Chains

JOÃO CAETANO^{a,b,c} AND THIAGO FLEURY^d

^a *Perimeter Institute for Theoretical Physics,
Waterloo, Ontario N2L 2Y5, Canada*

^b *Department of Physics and Astronomy & Guelph-Waterloo Physics Institute,
University of Waterloo, Waterloo, Ontario N2L 3G1, Canada*

^c *Centro de Física do Porto e Departamento de Física e Astronomia,
Faculdade de Ciências da Universidade do Porto,
Rua do Campo Alegre, 687, 4169-007 Porto, Portugal*

^d *Instituto de Física Teórica, UNESP - Univ. Estadual Paulista,
ICTP South American Institute for Fundamental Research,
Rua Dr. Bento Teobaldo Ferraz 271, 01140-070, São Paulo, SP, Brasil*

jd.caetano.s@gmail.com
tfleury@ift.unesp.br

Abstract

We compute three-point functions of general operators in the $\mathfrak{su}(1|1)$ sector of planar $\mathcal{N} = 4$ SYM in the weak coupling regime, both at tree-level and one-loop. Each operator is represented by a closed spin chain Bethe state characterized by a set of momenta parameterizing the fermionic excitations. At one-loop, we calculate both the two-loop Bethe eigenstates and the relevant Feynman diagrams for the three-point functions within our setup. The final expression for the structure constants is surprisingly simple and hints at a possible form factor based approach yet to be unveiled.

Contents

1	Introduction	1
2	Three-point functions at leading order	3
2.1	The one-loop Bethe eigenstates and structure constants	6
3	One-loop three-point functions	9
3.1	Two-loop coordinate Bethe eigenstates and Norms	9
3.2	One-loop perturbative calculation	11
3.3	Final result	14
4	Discussion and open problems	16
A	Notation and conventions	17
B	One-loop perturbative computation details	18
C	Some examples of three-point functions	24
C.1	Three half-BPS operators	24
C.2	Two non-BPS and one half-BPS operators	27
D	Wilson line contribution	30
D.1	Wilson line connecting two scalars	30
D.2	Wilson line connecting either a scalar and a fermion or two fermions . . .	31
E	A note on the $\mathfrak{su}(1 1)$ invariance of the final result	32

1 Introduction

Integrability has proven to be a powerful tool for studying the planar $\mathcal{N} = 4$ SYM theory. In particular, it was successfully used to compute all the two-point functions of the gauge-invariant single-trace operators for any value of the 't Hooft parameter λ , see for instance [1–3]. The predictions from integrability have been extensively tested and they correctly reproduce the known results obtained in perturbation theory at weak coupling and the ones obtained by the AdS/CFT conjecture in the strong coupling limit.

The natural next step is computing the three-point functions. Together with the two-point functions these are the building blocks for all the higher point correlators. With the help of table 1, let us briefly recall the state of the art concerning the computation of the three-point functions at weak coupling and explain where our findings fit within this picture.

A single-trace operator of $\mathcal{N} = 4$ SYM is thought of as a closed spin chain state. To leading order in the 't Hooft coupling these spin chain states are very well understood and given by the so-called Bethe ansatz. The problem at tree-level is purely combinatorial and amounts to *cutting* and *sewing* such spin chains. At the end of the day, this boils down to a computation of some scalar products of Bethe states. Nevertheless, this is a

Sector	Tree-level and Integrability	One-loop prescription	One-loop and Integrability	Higher loops
$\mathfrak{su}(2)$	[4], [5]	[6], [7]	[8], [9]	unknown
$\mathfrak{sl}(2)$	[10], [11]	[7] (some cases)	[10] (some cases)	unknown
$\mathfrak{su}(1 1)$	here	here	here	unknown
$\mathfrak{so}(6)$	[12] (some cases)	[6], [7]	unknown	unknown
$\mathfrak{psu}(2, 2 4)$	unknown	unknown	unknown	unknown

Table 1: The current status of the computation of three-point functions.

very rich and non-trivial problem. For instance, scalar products between Bethe states in higher rank algebras are not known. It is therefore so far unclear how to perform the computation of the most general $\mathfrak{psu}(2, 2|4)$ correlators as indicated by the last row of table 1.

This motivates one to start studying the rank one sectors in a systematic way. They consist of the $\mathfrak{su}(2)$, $\mathfrak{su}(1|1)$ and $\mathfrak{sl}(2)$ sectors and they played a very important role in the spectrum problem, see for instance [13]. The first three rows of the table 1 summarize the current knowledge on these sectors. In the $\mathfrak{su}(2)$ case, the final result for the structure constants turns out to be given in terms of determinants depending on three sets of numbers called Bethe rapidities while in the $\mathfrak{sl}(2)$ sector, it was found a formula given in terms of a sum over partitions of these Bethe rapidities. In this paper, we will study the remaining rank one sector.

Whichever sector we consider, there are, at one-loop, two effects that need to be taken into account.

Firstly, there is the two-loop correction to the Bethe state, which is of order λ and thus contributes to the one-loop structure constant. This amounts to correct not only the S -matrix but also modifying the Bethe ansatz itself by introducing the so-called contact terms. These are required due to the long-range nature of the dilatation operator which couples non-trivially neighboring magnons on the spin chain. In this regard, some surprises were found recently. The contact terms were found to be ultra-local in $\mathfrak{sl}(2)$ and much simpler than in the $\mathfrak{su}(2)$ case. In this paper we find a remarkably simple form for the contact terms in $\mathfrak{su}(1|1)$ allowing us to fully construct the two-loop Bethe state for an arbitrary number of magnons.

Secondly, there is the perturbative correction from the Feynman diagrams. This can be effectively described by an insertion of an operator at the splitting points of the spin chain and this is what we call the *prescription* for the one-loop computation. So far, the prescription was only fully computed for the $\mathfrak{so}(6)$ sector. For the $\mathfrak{sl}(2)$ sector, partial results were obtained in [7] but the complete computation remains to be done. In this paper, we provide the complete one-loop prescription for the $\mathfrak{su}(1|1)$ sector.

In the end, combining both loop contributions for $\mathfrak{su}(1|1)$, we found a strikingly simple formula for the one-loop structure constant C_{123} . Given three operators \mathcal{O}_i with N_i excitations with momenta $\{p_j^{(i)}\}_{j=1}^{N_i}$, and length L_i (the details of the exact setup will

be given below), we have

$$C_{123} = \mathcal{C} \frac{\prod_{i=1}^3 \prod_{j < k}^{N_i} \mathfrak{f}(y_j^{(i)}, y_k^{(i)})}{\prod_{i=1}^{N_1} \prod_{j=1}^{N_2} \mathfrak{f}(y_i^{(1)}, y_j^{(2)})} \prod_{k=1}^{N_1} \left[1 - (y_k^{(1)})^{L_2} \prod_{i=1}^{N_2} \left(-S(y_i^{(2)}, y_k^{(1)}) \right) \right], \quad (1.1)$$

where $y_j^{(i)} \equiv e^{ip_j^{(i)}}$, \mathcal{C} is a simple normalization factor given in (3.14), S is the $\mathfrak{su}(1|1)$ S -matrix. The most essential ingredient and main result of this work is the function \mathfrak{f} which is simply given by

$$\mathfrak{f}(s, t) = (s - t) \left[1 - \frac{g^2}{2} \left(\frac{s}{t} + \frac{t}{s} - \frac{1}{s} - s - \frac{1}{t} - t + 2 \right) + \mathcal{O}(g^4) \right], \quad (1.2)$$

with $g^2 = \frac{\lambda}{16\pi^2}$.

The paper is organized as follows. In section 2, we explain the three-point function setup that will be used in the remaining of the paper and compute the leading contribution to the structure constants in terms of a simple expression which is function of the momenta of the excitations. Section 3 is devoted to the calculation of the one-loop corrected structure constants. The section begins with the construction of the two-loop eigenstates by computing the contact terms, then we evaluate the relevant Feynman diagrams needed for determining the prescription for computing the one-loop corrections. In the end, we put the different contributions together and we arrive at the formula (1.1). Finally, the section 4 contains our conclusions and perspectives. Several Appendices have additional details omitted during the presentation.

2 Three-point functions at leading order

In this section, we perform the computation of the structure constants at leading order. The setup that will be used for the calculation involves composite operators made out of both fermionic and scalar fields. Each of these operators is thought of as a state of a closed spin chain with the fermionic fields being excitations over a ferromagnetic vacuum. The advantage of this approach is that the connection with the integrability tools of quantum spin chains becomes manifest (see for instance [2]) and facilitates the combinatorial problem.

The smallest (closed) sector of $\mathcal{N} = 4$ SYM containing both fermionic and bosonic fields is the $\mathfrak{su}(1|1)$. The field content of this sector consists of one complex scalar that we will denote as $Z = \Phi^{34}$ and a complex chiral fermion that shares with the scalar one R -charge index, for instance $\Psi = \psi_{\alpha=1}^4$. The setup for the calculation of the planar three-point functions that we will be considering involves an operator \mathcal{O}_1 given by a linear combination of single traces made out of products of these fields. More precisely,

$$\mathcal{O}_1 = \sum_{1 \leq n_1 < n_2 < \dots < n_{N_1} \leq L_1} \psi^{(1)}(n_1, n_2, \dots, n_{N_1}) \text{Tr} \left(Z \dots \underset{n_1}{\Psi} \dots \underset{n_2}{\Psi} \dots Z \right), \quad (2.1)$$

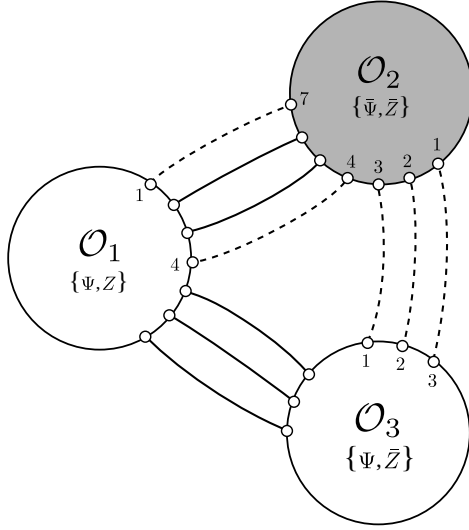


Figure 1: The leading order contribution to the three-point functions. The solid lines represent a bosonic propagator and the dashed lines represent a fermionic propagator. We also indicate our conventions for labeling the positions of the excitations. Notice that in our setup the first N_3 excitations of the operator \mathcal{O}_2 have always their position fixed.

where L_1 is the length of the operator, N_1 is the number of its fermionic fields and n 's are the positions of the excitations along the chain of Z 's. We designate the coefficients $\psi^{(1)}$ in this linear combination by wave-function. It is natural to consider the second operator \mathcal{O}_2 made out of the complex conjugate fields, namely

$$\mathcal{O}_2 = \sum_{1 \leq n_1 < n_2 < \dots < n_{N_2} \leq L_2} \psi^{(2)}(n_1, n_2, \dots, n_{N_2}) \text{Tr} \left(\bar{Z} \dots \bar{\Psi}_{n_1} \dots \bar{\Psi}_{n_2} \dots \bar{Z} \right). \quad (2.2)$$

In our conventions, the complex conjugate fields are given by

$$\begin{aligned} \bar{Z} &= (Z)^* = \Phi_{34} = \Phi^{12}, \\ \bar{\Psi} &= (\Psi)^\dagger = \bar{\psi}_{4, \dot{\alpha}=i}. \end{aligned} \quad (2.3)$$

From now on, we will omit the Lorentz spinorial indices at several places keeping in mind that they are always kept fixed.

As a consequence of the R -charge conservation, it is clear that we cannot take the third operator to be also in the same $\mathfrak{su}(1|1)$ sector to which \mathcal{O}_1 and \mathcal{O}_2 belong, if we want to have a non-vanishing result and avoid extremal correlation functions¹. Instead, we consider a “rotated” operator constructed by applying $\mathfrak{su}(4)$ generators several times to a $\mathfrak{su}(1|1)$ operator of the type \mathcal{O}_1 . The idea is to get a composite operator having a term with only Ψ and \bar{Z} fields in order to allow non-vanishing Wick contractions between all pairs of operators (see figure 1 for an example of a non-extremal three-point function).

¹The extremal case presents additional subtleties related to the mixing with double-trace operators, see [4]. We will not investigate such issues in this paper and therefore only non-extremal three-point functions will be considered.

More precisely, let us suppose that we start with a state made out of Ψ and Z fields. In order to convert a single Z into a \bar{Z} we must apply a pair of $\mathfrak{su}(4)$ generators that rotate its two R -charge indices. In sum, we can generate a term with Ψ 's and \bar{Z} 's by considering the following operation

$$\mathcal{O}_3 = \frac{1}{(L_3 - N_3)!^2} (\mathfrak{R}_4^2 \mathfrak{R}_3^1)^{L_3 - N_3} \sum_{1 \leq n_1 < \dots < n_{N_3} \leq L_3} \psi^{(3)}(n_1, \dots, n_{N_3}) \text{Tr} (Z \dots \Psi \dots \Psi \dots Z) , \quad (2.4)$$

where \mathfrak{R}_b^a are $\mathfrak{su}(4)$ generators and they act on the fields inside the trace. Now, the $\mathfrak{su}(4)$ generators may also act on the field Ψ which carries one R -charge index. Therefore, this operation will generate several terms coming from the different ways of acting with the generators,

$$\mathcal{O}_3 = \sum_{1 \leq n_1 < \dots < n_{N_3} \leq L_3} \psi^{(3)}(n_1, \dots, n_{N_3}) \left[\text{Tr} (\bar{Z} \dots \Psi \dots \Psi \dots \bar{Z}) + \right. \\ \left. + \text{Tr} (\bar{Z} \dots \psi^2 \dots \Psi \dots \Phi^{14}) + \dots \right] , \quad (2.5)$$

where in the first line we have the term where all the $\mathfrak{su}(4)$ generators act on the scalar fields Z . In the second line, we represent the terms where some of the generators also act on the fermionic fields Ψ . As an example of how the formula given above is evaluated consider,

$$(\mathfrak{R}_4^2 \mathfrak{R}_3^1) \cdot \text{Tr} (\Psi Z) = (\mathfrak{R}_4^2 \mathfrak{R}_3^1) \cdot \text{Tr} (\psi^4 \Phi^{34}) = \text{Tr} (\psi^2 \Phi^{14}) + \text{Tr} (\psi^4 \Phi^{12}) .$$

At tree-level, the terms in the second line of (2.5) do not give any contribution due to the R -charge conservation. In other words, one always has a zero Wick-contraction. Therefore, at leading order, only the first line contributes and we get a tree-level diagram of the type represented in figure 1. At one-loop, the terms in the second line will also need to be taken into account. We emphasize that the operators \mathcal{O}_1 in (2.1) and \mathcal{O}_3 in (2.4) are spinorial operators with N_1 and N_3 indices $\alpha = 1$ respectively. This follows from the definition of the field Ψ given previously. The operator \mathcal{O}_2 in (2.2) has N_2 Lorentz indices $\dot{\alpha} = \dot{1}$ associated to each of the fermions $\bar{\Psi}$.

In a conformal field theory, the two-point functions are completely fixed by the symmetries up to a normalization constant. For two operators having spinorial indices as shown below, we have

$$\langle \mathcal{O}_{i; 11 \dots 1_{N_i}}(x_1) \bar{\mathcal{O}}_{i; \dot{1} \dot{1} \dots \dot{1}_{N_i}}(x_2) \rangle = \mathcal{N}_i \frac{(J_{12, 1\dot{1}})^{N_i}}{|x_{12}|^{2\Delta_i}} , \quad (2.6)$$

where \mathcal{N}_i is a constant associated to the normalization of the operator, Δ_i is its conformal dimension and the tensorial structure is²

$$J_{ij, 1\dot{1}} = \frac{x_{ij}^\mu (\sigma_\mu^E)_{1\dot{1}}}{(2\pi)^2 |x_{ij}|} , \quad \text{with} \quad x_{ij}^\mu = x_i^\mu - x_j^\mu . \quad (2.7)$$

²See Appendix A for our conventions.

In the case of three-point functions of generic operators having spinorial indices, one has many inequivalent tensor structures consistent with the conformal symmetry, and the result of the correlation function is a linear combination of these structures. The constraints following from conformal symmetry on the higher point functions were studied for instance in [14–16]. However, for the setup considered in this work there is only one possible tensor and the three-point functions is of the form

$$\langle \mathcal{O}_{1;1_1\dots 1_{N_1}}(x_1) \mathcal{O}_{2;\dot{1}_1\dots \dot{1}_{N_2}}(x_2) \mathcal{O}_{3;1_1\dots 1_{N_3}}(x_3) \rangle = \frac{(J_{12,1\dot{1}})^{N_1} (J_{23,1\dot{1}})^{N_3} \sqrt{\mathcal{N}_1 \mathcal{N}_2 \mathcal{N}_3} C_{123}(g^2)}{|x_{12}|^{\Delta_1+\Delta_2-\Delta_3} |x_{13}|^{\Delta_1+\Delta_3-\Delta_2} |x_{23}|^{\Delta_2+\Delta_3-\Delta_1}}, \quad (2.8)$$

where we are considering $N_2 = N_1 + N_3$ and $g^2 = \frac{\lambda}{16\pi^2}$ with λ the 't Hooft parameter.

The structure constant $C_{123}(g^2)$ has a perturbative expansion when g^2 is small, and its leading order will be designated by $C_{123}^{(0)}$. Using the figure 1, we observe that the only non-trivial Wick contractions occur between operators \mathcal{O}_1 and \mathcal{O}_2 . The structure constant $C_{123}^{(0)}$ is then given by the product of the three wave-functions with a sum over the positions of the excitations between these two operators,

$$|C_{123}^{(0)}| = \alpha \left| \psi_{1,\dots,N_3}^{(3)} \sum_{N_3 < n_1 < \dots < n_{N_1} \leq L_2} \psi_{L_2+1-n_{N_1},\dots,L_2+1-n_1}^{(1)} \psi_{1,\dots,N_3,n_1,\dots,n_{N_1}}^{(2)} \right|. \quad (2.9)$$

α is a normalization factor that comes from the fact that we are normalizing the operators such that their two-point functions has the canonical form (2.6) with $\mathcal{N}_i = 1$. It is given by

$$\alpha = \sqrt{\frac{L_1 L_2 L_3}{\mathcal{N}^{(1)} \mathcal{N}^{(2)} \mathcal{N}^{(3)}}}, \quad \text{with } \mathcal{N}^{(j)} = \sum_{1 \leq n_1 < \dots < n_{N_j} \leq L_j} (\psi_{n_1,\dots,n_{N_j}}^{(j)})^* (\psi_{n_1,\dots,n_{N_j}}^{(j)}). \quad (2.10)$$

The main goal of this section is to find a closed formula for $C_{123}^{(0)}$.

2.1 The one-loop Bethe eigenstates and structure constants

To compute $C_{123}^{(0)}$ we must consider states with definite one-loop anomalous dimension [4]. The one-loop $\mathfrak{su}(1|1)$ integrable Hamiltonian and S -matrix can be found in [17, 13]. The Hamiltonian is simply the fermionic version of the Heisenberg Hamiltonian and it is written in terms of the Pauli matrices as

$$H_1 = 2g^2 \sum_{n=1}^L \left((1 - \sigma_n^3) - \frac{1}{2} (\sigma_n^1 \sigma_{n+1}^1 + \sigma_n^2 \sigma_{n+1}^2) \right), \quad (2.11)$$

where L is the length of the spin chain. At leading order the two-excitation S -matrix is independent of their momenta and simply given by

$$S(p_1, p_2) = -1. \quad (2.12)$$

In order to find the eigenstates of the Hamiltonian given above, we use the usual coordinate Bethe ansatz. A N -magnon state of a spin-chain of length L is of the form

$$|\psi_N\rangle = \sum_{1 \leq n_1 < n_2 < \dots < n_N \leq L} \psi_N(n_1, n_2, \dots, n_N) |n_1, \dots, n_N\rangle, \quad (2.13)$$

where the n_i 's in $|n_1, \dots, n_N\rangle$ indicate the position of the fermionic excitations Ψ on the chain (for details about the coordinate Bethe ansatz see [2, 4]). Notice that the ket $|n_1, \dots, n_N\rangle$ represents the trace in (2.1). The wave-function $\psi_N(n_1, \dots, n_N)$ is a combination of plane waves with as many terms as the number of possible permutations of the momenta with the relative coefficients being the S -matrices. Since the leading order $\mathfrak{su}(1|1)$ S -matrix is just -1 , the several terms in the wave-function will appear with alternating signs which we write as

$$\psi_N(n_1, n_2, \dots, n_N) = \sum_P \text{sign } P \exp(ip_{\sigma_P(1)}n_1 + ip_{\sigma_P(2)}n_2 + \dots + ip_{\sigma_P(N)}n_N) \quad (2.14)$$

where P indicates sum over all possible permutations σ_P of the elements $\{1, \dots, N\}$, and $\text{sign } P$ is the sign of the permutation. Moreover, we should impose the periodicity condition by requiring the momenta p_i to satisfy the Bethe equations

$$e^{ip_i L} = 1. \quad (2.15)$$

The cyclic property of the trace is implemented by imposing the zero momentum condition of the state,

$$\sum_{i=1}^N p_i = 2\pi \times \text{integer}. \quad (2.16)$$

Having determined the eigenstates of the one-loop $\mathfrak{su}(1|1)$ Hamiltonian, we can proceed to compute the leading order structure constant $C_{123}^{(0)}$ given in (2.9) by following some simple steps. First, we notice that since the positions of the excitations of the third operator are fixed, we can use (2.14) to write $\psi^{(3)}$ explicitly. It is simple to see that we obtain a Vandermonde determinant which can be also presented as a simple product,

$$\left| C_{123}^{(0)} \right| = \alpha \left| \prod_{j < k}^{N_3} \left[e^{ip_j^{(3)}} - e^{ip_k^{(3)}} \right] \sum_{N_3 < n_1 < \dots < n_{N_1} \leq L_2} (\psi_{n_1, \dots, n_{N_1}}^{(1)})^* \psi_{1, \dots, N_3, n_1, \dots, n_{N_1}}^{(2)} \right|. \quad (2.17)$$

Moreover we have replaced $\psi_{L_2+1-n_{N_1}, \dots, L_2+1-n_1}^{(1)}$ by $(\psi_{n_1, \dots, n_{N_1}}^{(1)})^*$ since they differ by at most a sign.

Notice that the first N_3 excitations of the wave-function $\psi^{(2)}$ have their positions fixed or *frozen*. In order to make the computation of this sum simpler, we consider an auxiliary problem where we add N_3 extra excitations to the wave-function $\psi^{(1)}$ and liberate the fixed N_3 roots of $\psi^{(2)}$ with their positions being summed over too,

$$\mathcal{S}_{aux} \equiv \sum_{1 \leq n_1 < \dots < n_{N_3+N_1} \leq L_2} (\psi_{n_1, \dots, n_{N_3+N_1}}^{(1)})^* \psi_{n_1, \dots, n_{N_3+N_1}}^{(2)}. \quad (2.18)$$

The advantage of considering this auxiliary problem is that the sum (2.18) can be easily computed due to the form of the wave-functions. Moreover, we can relate it with the original sum appearing in (2.17) as we now explain. Indeed, let us consider that N_3 momenta, say $\{p_1^{(1)}, \dots, p_{N_3}^{(1)}\}$, are complex. We can then dynamically localize the wave-function around the original N_3 positions by taking the limit of these momenta going to minus infinity. More precisely, we send $\{e^{-ip_1^{(1)}}, \dots, e^{-ip_{N_3}^{(1)}}\}$ to zero in such a way that

$$e^{-ip_1^{(1)}} \ll \dots \ll e^{-ip_{N_3}^{(1)}}. \quad (2.19)$$

Thus, given the explicit form of the wave-function (2.14), we observe that in this limit the sum over the positions of the extra roots in (2.18) is dominated by the term for which $n_1 = 1, \dots, n_{N_3} = N_3$. This procedure of sending roots to a particular limit in order to freeze their positions is the coordinate Bethe ansatz counterpart of the *freezing trick* used in [5] at the level of the six-vertex model. Neglecting all the subleading terms, we get that in this limit, (2.18) is reduced to

$$\mathcal{S}_{aux} \rightarrow \left(\prod_{k=1}^{N_3} e^{-ip_k^{(1)} k} \right) \sum_{N_3 < n_1 < \dots < n_{N_1} \leq L_2} (\psi_{n_1, \dots, n_{N_1}}^{(1)})^* \psi_{1, \dots, N_3, n_1, \dots, n_{N_1}}^{(2)}, \quad (2.20)$$

where we recognize precisely the original sum of (2.17).

Returning to our auxiliary problem, we use again that the wave-function is completely antisymmetric in its arguments to extend the limits of the sum (2.18). In compensation, we merely have to introduce a trivial overall combinatorial factor. Using the explicit form of the wave-function we write the sum (2.18) as

$$\mathcal{S}_{aux} = \frac{1}{N_2!} \sum_{\{n_i\}} \sum_{P, Q} \text{sign } P \text{ sign } Q \prod_{a=1}^{N_1+N_3} e^{(ip_{P(a)}^{(2)} - ip_{Q(a)}^{(1)})n_a}. \quad (2.21)$$

We emphasize again that we now sum without restrictions, $1 \leq n_i \leq L_2$, for all n_i . These sums over n_i can be explicitly computed as they are geometric series. Using the Bethe equations and the total momentum condition for the operator \mathcal{O}_2 , we can then simplify (2.21) to

$$\mathcal{S}_{aux} = \left[\prod_{a=1}^{N_1+N_3} \left(1 - e^{-ip_a^{(1)} L_2} \right) \right] \frac{1}{N_2!} \sum_{P, Q} \text{sign } P \text{ sign } Q \prod_{a=1}^{N_1+N_3} \frac{1}{e^{ip_{Q(a)}^{(1)}} - e^{ip_{P(a)}^{(2)}}}. \quad (2.22)$$

The remaining sum in the previous expression is manifestly the definition of a Cauchy determinant and, therefore, it can be written explicitly as a simple product as follows

$$\mathcal{S}_{aux} = \left[\prod_{a=1}^{N_1+N_3} \left(1 - e^{-ip_a^{(1)} L_2} \right) \right] \frac{\prod_{j < k} (e^{ip_j^{(1)}} - e^{ip_k^{(1)}})(e^{ip_k^{(2)}} - e^{ip_j^{(2)}})}{\prod_{j, k} (e^{ip_j^{(1)}} - e^{ip_k^{(2)}})}. \quad (2.23)$$

Notice that this expression contains as a limit the norm of an operator.³ It is given by

$$\mathcal{N}^{(j)} = L_j^{N_j}. \quad (2.24)$$

Finally, we take the limit of (2.23) when $\{e^{-ip_1^{(1)}}, \dots, e^{-ip_{N_3}^{(1)}}\}$ vanish as in (2.19). Plugging the resulting limit and taking into account the overall product multiplying the sum in (2.20), we obtain our final result

$$\left| C_{123}^{(0)} \right| = \left[\prod_{i=1}^3 L_i^{\frac{1-N_i}{2}} \right] \left[\prod_{j=1}^{N_1} \left(1 - e^{ip_j^{(1)} L_2} \right) \right] \frac{\prod_{a=1}^3 \prod_{j < k}^{N_a} (e^{ip_j^{(a)}} - e^{ip_k^{(a)}})}{\prod_{j=1}^{N_1} \prod_{k=1}^{N_2} (e^{ip_j^{(1)}} - e^{ip_k^{(2)}})} \quad (2.25)$$

It is now straightforward to confirm that our formula (1.1) given in the introduction, reduces to this one when g is set to zero.

This result fills the first column for the $\mathfrak{su}(1|1)$ row of the table 1 in the introduction. Let us remark that this expression is considerably simpler than the ones found for the $\mathfrak{su}(2)$ and $\mathfrak{sl}(2)$ sectors. This is perhaps not surprising given that at leading order we are dealing with a theory of free fermions so that the form of the $\mathfrak{su}(1|1)$ wave-function becomes quite simple. However, we will see that the one-loop result persists to be simpler than in the other sectors.

3 One-loop three-point functions

In this section, we compute the structure constants at first order in the 't Hooft coupling λ for our setup. There are two main ingredients in this computation. Firstly, one has to consider Bethe eigenstates that diagonalize the two-loop dilatation operator as these states are of order λ . Secondly, one has to compute the relevant Feynman diagrams at this order in perturbation theory. This second contribution can be compactly taken into account through the insertion of an operator at specific points of the spin chains as will be reviewed.

3.1 Two-loop coordinate Bethe eigenstates and Norms

The two-loop Bethe eigenstates are determined by diagonalizing the long-range Hamiltonian H [13]

$$H = H_1 + H_2, \quad (3.1)$$

where H_1 is given in (2.11) and

$$H_2 = 4g^2 \sum_{n=1}^L \left(2(\sigma_n^3 - 1) - \frac{1}{4}(\sigma_n^3 \sigma_{n+1}^3 - 1) + (\sigma_n^1 \sigma_{n+1}^1 + \sigma_n^2 \sigma_{n+1}^2) \left(\frac{9}{8} - \frac{1}{16} \sigma_{n+2}^3 \right) \right) \quad (3.2)$$

³If we set $N_3 = 0$ and consider $p_j^{(1)} \rightarrow p_j^{(2)}$ we get the expression for $\mathcal{N}^{(2)}$ after using the Bethe equations (2.15).

$$-\frac{1}{16}\sigma_n^3(\sigma_{n+1}^1\sigma_{n+2}^1+\sigma_{n+1}^2\sigma_{n+2}^2)-\frac{1}{8}\sigma_n^1(1+\sigma_{n+1}^3)\sigma_{n+2}^1-\frac{1}{8}\sigma_n^2(1+\sigma_{n+1}^3)\sigma_{n+2}^2\Big),$$

where σ^i are the Pauli matrices. In order to diagonalize it, we start with the usual coordinate Bethe ansatz which works when the excitations are at a distance bigger than the range of the interaction, i.e. when $|n_i - n_j| > 2$. In this region all we need is the two-loop S -matrix which reads

$$S(p_1, p_2) = -1 - 8ig^2 \sin\left(\frac{p_1}{2}\right) \sin\left(\frac{p_1 - p_2}{2}\right) \sin\left(\frac{p_2}{2}\right). \quad (3.3)$$

Given the long-range nature of the Hamiltonian (3.1), we expect the form of the wave-function to be modified with respect to the usual Bethe ansatz (2.14). In fact, when magnons are placed at neighboring positions on the spin chain they interact in a non-trivial way. Therefore, the wave-function must be refined by the inclusion of the so-called *contact terms*. For instance, in the case of three magnons we write it as

$$\psi(n_1, n_2, n_3) = \phi_{123} + \phi_{213}S_{21} + \phi_{132}S_{32} + \phi_{312}S_{31}S_{32} + \phi_{231}S_{31}S_{21} + \phi_{321}S_{32}S_{31}S_{21},$$

where we have used the notation $S_{ab} = S(p_a, p_b)$ and

$$\begin{aligned} \phi_{abc} = e^{ip_a n_1 + ip_b n_2 + ip_c n_3} & \left(1 + g^2 \mathbb{C}(p_a, p_b) \delta_{n_2, n_1+1} \delta_{n_3 > n_2+1} + g^2 \mathbb{C}(p_b, p_c) \delta_{n_2 > n_1+1} \delta_{n_3, n_2+1} \right. \\ & \left. + g^2 \mathbb{C}(p_a, p_b, p_c) \delta_{n_2, n_1+1} \delta_{n_3, n_2+1} \right). \end{aligned} \quad (3.4)$$

The functions \mathbb{C} are the contact terms which are fixed by solving the energy eigenvalue problem. In the case of N -magnons, the wave-function has a similar structure. It consists of $N!$ terms coming from the permutations of $\{p_1, \dots, p_N\}$ and $N - 1$ types of contact terms namely $\mathbb{C}(p_i, p_j), \dots, \mathbb{C}(p_1, \dots, p_N)$.

Unexpectedly, we have found that up to seven magnons the contact terms are simply given by⁴

$$\mathbb{C}(p_1, \dots, p_N) = \frac{N - 1}{2}. \quad (3.5)$$

Even though we have not proved the validity of this formula for an arbitrarily high number of magnons, the pattern emerging up to seven magnons is quite suggestive. Given the form of the contact terms in the $\mathfrak{su}(2)$ and $\mathfrak{sl}(2)$ sectors, the simplicity of the $\mathfrak{su}(1|1)$ result is quite surprising. In particular, notice that they are independent of the momenta of the colliding magnons. This might be pointing towards the existence of a new algebraic description of these states yet to be unveiled.

As already explained, in order to correctly compute the three-point functions we need to know the norm of the Bethe eigenstates as we are normalizing the result by the two-point functions. Remarkably, we have checked numerically up to six-magnons that the two-loop (coordinate) norm is given by

$$\mathcal{N} = \det_{j,k \leq N} \frac{\partial}{\partial p_j} \left[Lp_k + \frac{1}{i} \sum_{m \neq k}^N \log S(p_m, p_k) \right]. \quad (3.6)$$

⁴We thank Tianheng Wang for collaboration on this point.

Interestingly, this formula is precisely the well-known Gaudin norm for the one-loop $\mathfrak{su}(2)$ Bethe states. Still within the $\mathfrak{su}(2)$ sector, it was recently shown in [8] that this expression remains valid at higher loops leading to an all-loop conjecture for the norm. Moreover, the two-loop norm for $\mathfrak{sl}(2)$ Bethe states was found to be precisely of the type (3.6) as described in [10]. In all these cases, the contact terms recombine exactly to preserve the determinant form. This is very suggestive of an underlying hidden structure that is worth investigating.

3.2 One-loop perturbative calculation

Loop computations will give rise to divergences which require the introduction of a regularization scheme. A very convenient one and the one that will be used in this work is the *point splitting* regularization. At one-loop, only neighboring fields inside any of the single-trace operators interact and the divergences arise because the two fields are at the same spacetime point. The idea behind the point splitting regularization is to separate these two fields by a distance ϵ which will act as a regulator⁵.

Consider a $\mathfrak{su}(1|1)$ bare operator which is an eigenstate of the one-loop dilatation operator. Its non-vanishing two-point function is of the form

$$\langle \mathcal{O}_{i;1_1\dots 1_{N_i}}(x_1) \bar{\mathcal{O}}_{i;\bar{1}_1\dots \bar{1}_{N_i}}(x_2) \rangle = \mathcal{N}_i \frac{(J_{12,1\bar{1}})^{N_i}}{|x_{12}|^{2\Delta_{0,i}}} \left(1 + 2g^2 a_i - \gamma_i \log \left(\frac{x_{12}^2}{\epsilon^2} \right) \right), \quad (3.7)$$

where the tensor on the right-hand side was defined in (2.7). In the expression above, $\Delta_{0,i}$ and γ_i are the free scaling dimension and the one-loop anomalous dimension of the operator \mathcal{O}_i respectively, \mathcal{N}_i is a normalization constant and a_i is a scheme dependent constant. In addition, the three-point function of three $\mathfrak{su}(1|1)$ bare operators that diagonalize the one-loop dilatation operator is, in our setup, fixed by conformal symmetry and takes the form (see [6] for details)

$$\langle \mathcal{O}_{1;1_1\dots 1_{N_1}}(x_1) \mathcal{O}_{2;\bar{1}_1\dots \bar{1}_{N_2}}(x_2) \mathcal{O}_{3;1_1\dots 1_{N_3}}(x_3) \rangle = \quad (3.8)$$

$$\frac{(J_{12,1\bar{1}})^{N_1} (J_{23,1\bar{1}})^{N_3} \sqrt{\mathcal{N}_1 \mathcal{N}_2 \mathcal{N}_3}}{|x_{12}|^{\Delta_{0,1}+\Delta_{0,2}-\Delta_{0,3}} |x_{13}|^{\Delta_{0,1}+\Delta_{0,3}-\Delta_{0,2}} |x_{23}|^{\Delta_{0,2}+\Delta_{0,3}-\Delta_{0,1}}} C_{123}^{(0)} \times$$

$$\left(1 + g^2 (C_{123}^{(1)} + a_1 + a_2 + a_3) - \frac{\gamma_1}{2} \log \left(\frac{x_{12}^2 x_{13}^2}{x_{23}^2 \epsilon^2} \right) - \frac{\gamma_2}{2} \log \left(\frac{x_{12}^2 x_{23}^2}{x_{13}^2 \epsilon^2} \right) - \frac{\gamma_3}{2} \log \left(\frac{x_{23}^2 x_{13}^2}{x_{12}^2 \epsilon^2} \right) \right)$$

where we have factored out the tree-level constant $C_{123}^{(0)}$.

To extract the regularization scheme independent structure constant $C_{123}^{(1)}$ from the expression above, we have to divide the three-point function by the square root of the

⁵In order to preserve the gauge invariance, one can introduce a Wilson line between the two shifted fields. This will in principle introduce extra diagrams at one-loop, coming from the gluon emission from the Wilson line. However, we will show in the Appendix D that this additional contribution actually vanishes at this order in perturbation theory.

$$\text{Diagram} - \frac{1}{2} \text{Diagram} - \frac{1}{2} \text{Diagram} = 0$$

Figure 2: The wavy-line in the figure is just a representation of a one-loop diagram (for example, a gluon exchange). When the contribution of the square root of the two-point functions is subtracted (this is the reason for the factor $\frac{1}{2}$), all the diagrams involving just two operators are canceled.

$$\text{Diagram} - \frac{1}{2} \text{Diagram}$$

Figure 3: A genuine three-point diagram to which we subtract half of the same diagram but seen as a two-point process is shown. The constant coming from this combination of diagrams is regularization scheme and normalization independent.

two-point functions of all the operators to get rid of the constants a_i 's. After performing this division, one can then read the meaningful structure constant.

From the Feynman diagrams computation point of view, it is actually simpler to calculate $C_{123}^{(1)}$ instead of the combination $(C_{123}^{(1)} + a_1 + a_2 + a_3)$. In fact, because we have to divide by the square root of the two-point functions, all one-loop diagrams in the three-point function involving only two operators are canceled. The figure 2 has an example of a such cancellation.

The conclusion is that one is left with the computation of only genuine three-point diagrams, i.e., the diagrams involving fields from the three operators⁶. The allowed positions of the spin chains where it is possible to have those genuine diagrams are commonly called the *splitting points*. We are then seeking the constants coming from the genuine three-point diagrams subtracted by the constants coming from the same diagrams but now seen as two-point processes. This is exemplified in the figure 3.

The details of the Feynman diagram computation are given in the Appendix B and here we just provide the results. In the figure 4, we list all diagrams giving a non-zero contribution to the three-point functions as well as the result of the respective scheme independent constants. A relevant aspect of this computation is that some terms in the second line of (2.5) are now important at one-loop level. Indeed, from figure 4 we realize that the second graph of the second row mixes up the R -charge indices of the scalar and the fermion. In particular, the scalar Φ^{14} and the fermion ψ^2 in the second line of (2.5)

⁶This fact was dubbed the *slicing argument* in [7]

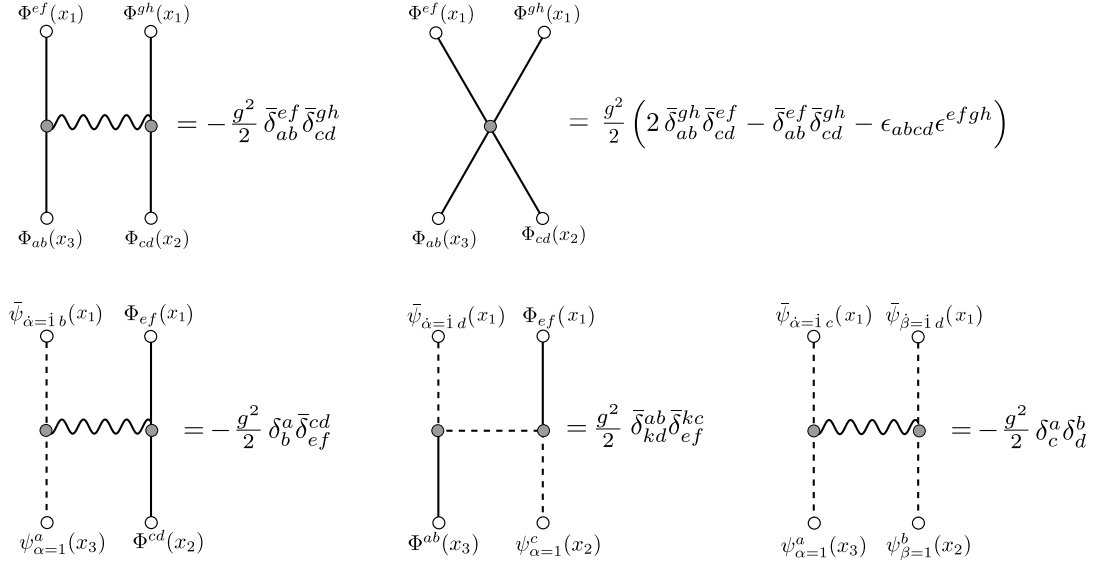


Figure 4: These are the relevant one-loop diagrams for the three-point functions. All other graphs give a zero contribution. The solid, wiggly and dashed lines represent the scalars, gluons and fermions, respectively. The constants are obtained by combining the three-point and two-point graphs as illustrated in figure 3. We have used the point splitting regularization and the Feynman gauge. For three-point diagrams we take the limit where a pair of dots (either top or bottom) are brought to the same spacetime points. For the two-point function, both pairs of dots (top and bottom) are brought to the same spacetime points. We are using the definition $\bar{\delta}_{cd}^{ab} \equiv \delta_c^a \delta_d^b - \delta_c^b \delta_d^a$.

can be converted into a Ψ and a \bar{Z} through this diagram. The resulting state can then be contracted with the remaining external operators and give a non-vanishing contribution.

From the results of figure 4, we can directly read off an operator acting on the two fields at the splitting points of an external state and that gives those same constants after contraction with the remaining states. We denote this operator by \mathcal{F} and define it by the following matrix elements

$$\langle \psi^a \psi^b | \mathcal{F} | \psi^c \psi^d \rangle = -\delta^{ac} \delta^{bd}, \quad (3.9)$$

$$\langle \Phi^{ef} \Phi^{gh} | \mathcal{F} | \Phi^{ab} \Phi^{cd} \rangle = 2 \bar{\delta}^{gh,ab} \bar{\delta}^{ef,cd} - 2 \bar{\delta}^{ef,ab} \bar{\delta}^{gh,cd} - \epsilon^{abcd} \epsilon^{efgh},$$

$$\langle \Phi^{de} \psi^f | \mathcal{F} | \Phi^{ab} \psi^c \rangle = -\delta^{fc} \bar{\delta}^{ab,de}, \quad \langle \psi^f \Phi^{de} | \mathcal{F} | \psi^c \Phi^{ab} \rangle = -\delta^{fc} \bar{\delta}^{ab,de},$$

$$\langle \Phi^{de} \psi^f | \mathcal{F} | \psi^c \Phi^{ab} \rangle = \delta^{ce} \bar{\delta}^{ab,df}, \quad \langle \psi^f \Phi^{de} | \mathcal{F} | \Phi^{ab} \psi^c \rangle = \delta^{ce} \bar{\delta}^{ab,df},$$

where $\bar{\delta}^{ab,cd} \equiv \delta^{ac} \delta^{bd} - \delta^{ad} \delta^{bc}$ and in the second line we recognize the $\mathfrak{so}(6)$ Hamiltonian [18, 7, 6]. It is simple to check that the operator $\frac{g^2}{2} \mathcal{F}$ reproduces the constants of figure 4.

For the specific setup that we are considering only the diagrams of figure 4 are relevant, since additional diagrams either cancel among them or vanish, see Appendix B for details. In the case of a more general setup, the operator \mathcal{F} defined receives corrections from new diagrams.

In what follows, the operator \mathcal{F} will appear with additional indices as \mathcal{F}_{ij} , which indicate the sites in the spin chain where the operator acts. As an example, we have that

$$\langle \dots \bar{\Psi}^i \bar{Z}^j \dots | \frac{g^2}{2} \mathcal{F}_{ij} | \dots \bar{\Psi}^i \bar{Z}^j \dots \rangle = -\frac{g^2}{2},$$

which reproduces the result of the first diagram of the second row of figure 4. It is important to note that when the operator \mathcal{F}_{ij} acts on non-neighboring sites, it can pick up additional minus signs due to statistics, for example,

$$\langle \Psi \dots \underbrace{\Psi \dots \Psi}_{n \text{ fermions}} \dots Z | \frac{g^2}{2} \mathcal{F}_{1L} | Z \dots \underbrace{\Psi \dots \Psi}_{n \text{ fermions}} \dots \Psi \rangle = (-1)^n \frac{g^2}{2},$$

where n denotes the number of fermionic excitations between the first and last sites and we have used the last rule of (3.9).

3.3 Final result

We now give the complete expression for the structure constants up to one-loop in the setup considered in this work. It reads

$$\begin{aligned} C_{123} = \alpha \times & \left(\langle \mathbf{1}^f | 1 + \frac{g^2}{2} \mathcal{F}_{L_3-N_3, L_3-N_3+1} + \frac{g^2}{2} \mathcal{F}_{L_1,1} | \underbrace{\bar{Z} \dots \bar{Z}}_{L_3-N_3} i_1 \dots i_{L_2-N_3} \rangle \right. \\ & \left. \langle \underbrace{\bar{\Psi} \dots \bar{\Psi}}_{N_3} i_1 \dots i_{L_2-N_3} | 1 + \frac{g^2}{2} \mathcal{F}_{N_3, N_3+1} + \frac{g^2}{2} \mathcal{F}_{L_2,1} | \mathbf{2} \rangle \right) \times \\ & \left. \langle \underbrace{\Psi \dots \Psi}_{N_3} \underbrace{\bar{Z} \dots \bar{Z}}_{L_3-N_3} | 1 + \frac{g^2}{2} \mathcal{F}_{N_3, N_3+1} + \frac{g^2}{2} \mathcal{F}_{L_3,1} | \mathbf{3} \rangle \right), \end{aligned} \quad (3.10)$$

where we have that

$$\alpha = \sqrt{\frac{L_1 L_2 L_3}{\mathcal{N}^{(1)} \mathcal{N}^{(2)} \mathcal{N}^{(3)}}}, \quad (3.11)$$

with $\mathcal{N}^{(i)}$ being the respective norms and we are using the conventions

$$\langle \sigma_{i_1} \sigma_{i_2} \dots \sigma_{i_L} | \sigma_{j_1} \sigma_{j_2} \dots \sigma_{j_L} \rangle = \delta_{i_1 j_1} \delta_{i_2 j_2} \dots \delta_{i_L j_L},$$

where σ is any field.

In the formula (3.10), i_a can be either \bar{Z} or $\bar{\Psi}$ and a sum over all these intermediate states is implied. Moreover, we have included a superscript f in the bra associated

to the operator \mathcal{O}_1 to emphasize that the state was *flipped*⁷, see [4] for details. The external states are the two-loop corrected Bethe eigenstates as described in section 3.1, for instance

$$|1\rangle = |1\rangle^{(0)} + g^2 |1\rangle^{(1)} + \mathcal{O}(g^4). \quad (3.12)$$

We have checked that for the simple case of three half-BPS operators, the one-loop correction to the structure constant vanishes as expected from the non-renormalization theorem of [19], see Appendix C for details. Additionally, in the Appendix E we check that this result satisfies some constraints from symmetry considerations.

The expression (3.10) can now be evaluated as an explicit function of the Bethe roots by using the known form of the two-loop Bethe states. As the number of excitations on the external states increases, such task becomes tedious and the result gets lengthy obscuring possible simplifications. Nevertheless, we can easily deal with states of arbitrary length but only a few magnons. It turns out that the manipulation of the resulting expressions for these simple cases reveals a strikingly compact structure that can be easily generalizable for arbitrary complicated states. We then resort to the numerical approach in order to confirm that such generalization actually holds. In the end, we find a formula given by a very simple and natural deformation of the tree-level result (2.25), as follows

$$C_{123} = \mathcal{C} \frac{\prod_{k=1}^3 \prod_{i < j}^{N_k} \mathfrak{f}(y_i^{(k)}, y_j^{(k)})}{\prod_{i=1}^{N_1} \prod_{j=1}^{N_2} \mathfrak{f}(y_i^{(1)}, y_j^{(2)})} \prod_{k=1}^{N_1} \left[1 - (y_k^{(1)})^{L_2} \prod_{i=1}^{N_2} \left(-S(y_i^{(2)}, y_k^{(1)}) \right) \right], \quad (3.13)$$

where we are using the notation $y_k^{(i)} = e^{ip_k^{(i)}}$ and the normalization factor \mathcal{C} is given by

$$\mathcal{C} = \sqrt{\frac{L_1 L_2 L_3}{\mathcal{N}^{(1)} \mathcal{N}^{(2)} \mathcal{N}^{(3)}}} \left[1 + g^2 (N_3^2 - 1) - \frac{1}{4} \sum_{i=1}^3 \gamma_i \right], \quad (3.14)$$

with γ_i being the anomalous dimension of the operator \mathcal{O}_i . As described in the section 3.1, the norms $\mathcal{N}^{(i)}$ are given by the formula

$$\mathcal{N}^{(i)} = \det_{j, k \leq N_i} \frac{\partial}{\partial p_j^{(i)}} \left[L p_k^{(i)} + \frac{1}{i} \sum_{m \neq k}^{N_i} \log S(p_m^{(i)}, p_k^{(i)}) \right]. \quad (3.15)$$

The most important and non-trivial part of the final result is the function \mathfrak{f} which reads

$$\mathfrak{f}(s, t) = (s - t) \left[1 - \frac{g^2}{2} \left(\frac{s}{t} + \frac{t}{s} - \frac{1}{s} - s - \frac{1}{t} - t + 2 \right) \right]. \quad (3.16)$$

⁷In short, the *flipping* operation $\mathcal{F}l$ introduced in [4] is defined as $\mathcal{F}l: \psi(n_1, \dots, n_N) |n_1, \dots, n_N\rangle \mapsto \psi(n_1, \dots, n_N) \langle L - n_N + 1, \dots, L - n_1 + 1 | \hat{C}$, where \hat{C} means charge conjugation which exchanges $Z \leftrightarrow \bar{Z}$ and $\Psi \leftrightarrow \bar{\Psi}$.

The momenta $p_k^{(j)}$ of the fermionic excitations must satisfy the Bethe equations which take the form

$$e^{ip_k^{(j)}L_j} = \prod_{i \neq k}^N \left(-S(p_k^{(j)}, p_i^{(j)}) \right), \quad (3.17)$$

and the total momentum condition (2.16). This constitutes the most important result of this paper and it will be discussed in the next section.

4 Discussion and open problems

In this work, we have computed both the leading order contribution and the one-loop perturbative correction at weak coupling to the three-point functions of single-trace operators of $\mathcal{N} = 4$ SYM in the $\mathfrak{su}(1|1)$ sector. The $\mathfrak{su}(1|1)$ sector is closed to all orders in perturbation theory [17] and it is the simplest sector having both fermions and bosons. Representing each operator by a Bethe eigenstate, we were able to derive a simple expression (2.25) for the leading order result in terms of the momenta characterizing the states.

In addition, we have also computed the one-loop correction by evaluating the relevant Feynman diagrams and also determining the two-loop Bethe eigenstates and their norm. The prescription for computing the scheme independent three-point structure constant turns out to be given in terms of the insertion of the operator \mathcal{F} , defined in (3.9), at the splitting points of the spin chains.

Regarding the external states, due to the long-range property of the two-loop dilatation operator in the $\mathfrak{su}(1|1)$ sector, its diagonalization involves the usual Bethe ansatz corrected by the contact terms. These in turn are independent of the momenta of the excitations and have a very simple expression for an arbitrary number of magnons, see (3.5). The norm of these states is compactly given by a simple determinant, analogous to the well known case of the $\mathfrak{su}(2)$ sector.

The one-loop structure constant in our setup turns out to be given by the simple formula (3.13) in terms of the Bethe roots. It is tempting to investigate the thermodynamic limit of our result, namely when we consider one or more long spin chains $L_i \gg 1$, with a large number of excitations $N_i = \mathcal{O}(L_i)$. This might be useful for future comparison with string theory calculations in a specific limit. An obvious open problem is the computation of the three-point functions in higher rank sectors at least at tree-level. Our result and the results of [5, 10] are encouraging in order to find a simple expression for the full $\mathfrak{psu}(2, 2|4)$. The main obstacle is the knowledge of the scalar products of Bethe states for generic (super) algebras, although some progress has been made in the $\mathfrak{su}(3)$ case [20–23].

The final expression (3.13) is very suggestive and deserves further comments. Apart from the simple normalization factor \mathcal{C} given by the expression (3.14), the structure constant has two distinct contributions. Firstly, the one-loop correction to the S -matrix appears in a very natural way when we look at the tree-level result (2.25). Secondly, the most non-trivial part comes from the function \mathfrak{f} . The one-loop result is achieved by deforming this function, which bears some similarities to the $\mathfrak{su}(2)$ and $\mathfrak{sl}(2)$ cases [8, 10].

As already pointed out in [10], it would be interesting to deepen the connection of the three-point function with form factors as started in [24,25]. In particular, that could shed light on a (non-perturbative) definition of the function \mathfrak{f} from the form factors axioms. In fact, such axiomatic approach was recently explored in the context of the scattering amplitudes [26–28]. There, the central object called pentagon transition $P(u|v)$ was required to satisfy some natural constraints from the integrability point of view. These conditions were then used to bootstrap the function exactly. In this regard, we notice some striking similarities of the dependence of our final result on this function \mathfrak{f} with the expression (9) of [26] which corresponds to a multi-particle transition. We hope that such ideas can be applied for the calculation of three-point functions at any value of the coupling constant.

Acknowledgements

We would like to thank P. Vieira for many invaluable discussions and suggestions. We also thank B. Basso, N. Berkovits, N. Gromov, Y. Jiang, H. Nastase, J. Penedones, D. Serban, A. Sever, C. Sieg, E. Sobko, J. Toledo for comments and discussions and especially T. Wang for collaboration in a stage of this project. We would like to thank the warm hospitality of the ICTP-SAIFR, FAPESP grant 2011/11973-4, where part of this work was done. TF would like to thank the warm hospitality of the Perimeter Institute where this work was initiated.

JC is funded by the FCT fellowship SFRH/BD/69084/2010. This work has been supported in part by the Province of Ontario through ERA grant ER 06-02-293. Research at the Perimeter Institute is supported in part by the Government of Canada through NSERC and by the Province of Ontario through MRI. This work was partially funded by the research grants PTDC/FIS/099293/2008 and CERN/FP/116358/2010. *Centro de Física do Porto* is partially funded by FCT under grant PEst-OE/FIS/UI0044/2011. TF would like to thank FAPESP grant 2013/12416-7 and 2009/50775-3 for financial support.

A Notation and conventions

In this Appendix, we fix our conventions for the perturbative computations. The $\mathcal{N} = 4$ SYM with $SU(N)$ gauge group has the following Lagrangian [29, 30]

$$\begin{aligned} \mathcal{L} = \text{Tr} \Big(& -\frac{1}{2} F_{\mu\nu} F^{\mu\nu} + 2 \mathcal{D}_\mu \Phi_{ab} \mathcal{D}^\mu \Phi^{ab} + 2i \psi^{\alpha a} \sigma_{\alpha\dot{\alpha}}^\mu (\mathcal{D}_\mu \bar{\psi}_a)^{\dot{\alpha}} \\ & + 2g_{\text{YM}}^2 [\Phi^{ab}, \Phi^{cd}] [\Phi_{ab}, \Phi_{cd}] - 2\sqrt{2} g_{\text{YM}} ([\psi^{\alpha a}, \Phi_{ab}] \psi_\alpha^b - [\bar{\psi}_{\dot{\alpha} a}, \Phi^{ab}] \bar{\psi}_{\dot{b}}^{\dot{\alpha}}) \Big), \end{aligned} \quad (\text{A.1})$$

with all the fields in the adjoint representation of the gauge group and the covariant derivative is $\mathcal{D}_\mu \cdot = \partial_\mu - ig_{\text{YM}} [A_\mu, \cdot]$. The propagators extracted from this Lagrangian are (we are suppressing the gauge indices and taking the leading order in N)

$$\langle \Phi^{ab}(x) \Phi_{cd}(0) \rangle = \frac{\bar{\delta}_{cd}^{ab}}{8} \frac{1}{(2\pi)^2 (-x^2 + i\epsilon)},$$

$$\begin{aligned}\langle \psi_\alpha^a(x) \bar{\psi}_{\dot{\beta}b}(0) \rangle &= \frac{i \delta_b^a}{2} \sigma_{\alpha\dot{\beta}}^\mu \partial_\mu \frac{1}{(2\pi)^2(-x^2 + i\epsilon)}, \\ \langle A_\mu(x) A_\nu(0) \rangle &= -\frac{\eta_{\mu\nu}}{2} \frac{1}{(2\pi)^2(-x^2 + i\epsilon)},\end{aligned}$$

where $\bar{\delta}_{cd}^{ab} \equiv \delta_c^a \delta_d^b - \delta_c^b \delta_d^a$. We are using the Minkowski metric $(+ - - -)$ and the Feynman gauge. The action of the (classical) supersymmetry generators are given by [31]

$$\begin{aligned}[\mathfrak{Q}_a^\alpha, \Phi^{bc}] &= \frac{i\sqrt{2}}{2} (\delta_a^b \psi^{\alpha c} - \delta_a^c \psi^{\alpha b}), \\ [\mathfrak{Q}_a^\alpha, \psi_\beta^b] &= \delta_a^b F_\beta^\alpha, \\ [\mathfrak{Q}_a^\alpha, \bar{\psi}_b^{\dot{\beta}}] &= 2\sqrt{2} \mathcal{D}^{\dot{\beta}\alpha} \Phi_{ab},\end{aligned}$$

and the conjugate expressions for the action of $\bar{\mathfrak{Q}}_{\dot{\alpha}}$. The action of the R -symmetry generators is given by

$$\begin{aligned}[\mathfrak{R}_b^a, \Phi^{cd}] &= \delta_b^c \Phi^{ad} + \delta_b^d \Phi^{ca} - \frac{1}{2} \delta_b^a \Phi^{cd}, \\ [\mathfrak{R}_b^a, \psi^c] &= \delta_b^c \psi^a - \frac{1}{4} \delta_b^a \psi^c.\end{aligned}$$

In the computations of the Feynman diagrams, in particular for the evaluation of the integrals, we analytically continued to Euclidean space by using

$$x^0 = ix^4, \quad \sigma_M^0 = -\sigma_E^0, \quad \sigma_M^i = i\sigma_E^i,$$

where the subscripts M means Minkowski space and E means Euclidean space,

$$\sigma_M^0 = \text{Id}_{2 \times 2},$$

and, finally, σ_M^i are the usual Pauli matrices.

B One-loop perturbative computation details

In this Appendix, we present the details of the perturbative computation of the three-point functions at one-loop using the point splitting regularization. As reviewed in the main part of this paper, in order to obtain scheme and normalization independent structure constants we also need to know the results of the two-point functions. For completeness, we explicitly compute the one-loop dilatation operator of the $\mathfrak{su}(1|1)$ sector as well.

Typically three kinds of integrals will appear in the computations

$$\begin{aligned}Y_{123} &= \int d^4u I_{x_1u} I_{x_2u} I_{x_3u}, \\ X_{1234} &= \int d^4u I_{x_1u} I_{x_2u} I_{x_3u} I_{x_4u},\end{aligned}$$

Figure 5 shows four rows of Feynman diagrams and their corresponding mathematical expressions. The diagrams use solid, wiggly, and dashed lines to represent scalars, gluons, and fermions, respectively. The expressions involve various integrals and tensors.

Row 1: $\Phi^{ef}(x_4) \Phi^{gh}(x_1) \text{ (wavy)} = -\frac{\lambda}{128} F_{12,34} I_{x_1 x_2} I_{x_3 x_4} \bar{\delta}_{ab}^{ef} \bar{\delta}_{cd}^{gh}$

Row 2: $\Phi^{ef}(x_4) \Phi^{gh}(x_1) \text{ (dashed)} = \frac{\lambda}{128} X_{1234} \left(2 \bar{\delta}_{ab}^{gh} \bar{\delta}_{cd}^{ef} - \bar{\delta}_{ab}^{ef} \bar{\delta}_{cd}^{gh} - \epsilon_{abcd} \epsilon^{efgh} \right)$

Row 3: $\Phi^{cd}(x_2) \Phi^{ab}(x_1) \text{ (shaded)} = \text{wavy} + \text{scalloped} + \text{solid} + \text{dashed} = -\frac{\lambda}{4} Y_{112} \bar{\delta}_{ab}^{cd}$

Row 4: $\bar{\psi}_{\dot{\alpha}=1 b}(x_4) \Phi_{ef}(x_1) \text{ (shaded)} = \text{wavy} + \text{dashed} = -2\lambda \sigma_{E\alpha\dot{\alpha}}^{\mu} \partial_{2,\mu} Y_{112} \delta_b^a$

Row 5: $\bar{\psi}_{\dot{\alpha}=1 d}(x_4) \Phi_{ef}(x_1) \text{ (dashed)} = \frac{\lambda}{16} \sigma_{E\alpha\dot{\alpha}}^{\mu} \left(\partial_{4,\mu} \partial_2 \cdot \partial_3 - \partial_{3,\mu} \partial_2 \cdot \partial_4 - \partial_{2,\mu} \partial_3 \cdot \partial_4 - \partial_{3,\mu} \partial_1 \cdot \partial_4 - \partial_{4,\mu} \partial_1 \cdot \partial_3 \right) H_{12,34} \bar{\delta}_{cd}^{ab} \bar{\delta}_{ef}^{kc}$

Row 6: $\bar{\psi}_{\dot{\alpha}=1 c}(x_4) \bar{\psi}_{\dot{\beta}=1 d}(x_1) \text{ (wavy)} = \frac{\lambda}{4} \sigma_{E\alpha\dot{\alpha}}^{\mu} \sigma_{E\beta\dot{\beta}}^{\nu} \left(\partial_{2,\nu} \partial_{4,\mu} \partial_1 \cdot \partial_3 + \partial_{1,\nu} \partial_{3,\mu} \partial_2 \cdot \partial_4 - \partial_{1,\mu} \partial_{2,\nu} \partial_3 \cdot \partial_4 - \partial_{3,\mu} \partial_{4,\nu} \partial_1 \cdot \partial_2 \right) H_{12,34} \delta_c^a \delta_d^b$

Figure 5: The results of the Feynman diagrams computation omitting both terms that must vanish or cancel when summing all the diagrams (see text) and factors of N . The solid, wiggly and dashed lines represent the scalars, gluons and fermions, respectively. The $\bar{\delta}$ was defined in Appendix A.

$$H_{12,34} = \int d^4u d^4v I_{x_1 u} I_{x_2 u} I_{uv} I_{x_3 v} I_{x_4 v} ,$$

where $I_{x_a x_b}$ is the (euclidean) scalar propagator defined as

$$I_{x_a x_b} \equiv \frac{1}{(2\pi)^2 (x_a - x_b)^2} .$$

The Y and X integrals are well-known and explicit expressions for them can be found for instance in [32, 7]. The integral H is not known analytic, however, only its derivatives will be needed. In particular, the following combination [32] turns out to be useful

$$F_{12,34} \equiv \frac{(\partial_1 - \partial_2) \cdot (\partial_3 - \partial_4) H_{12,34}}{I_{x_1 x_2} I_{x_3 x_4}} \quad (\text{B.1})$$

$$= \frac{X_{1234}}{I_{x_1 x_3} I_{x_2 x_4}} - \frac{X_{1234}}{I_{x_1 x_4} I_{x_2 x_3}} + G_{1,34} - G_{2,34} + G_{3,12} - G_{4,12},$$

where

$$G_{a,bc} = \frac{Y_{abc}}{I_{x_a x_c}} - \frac{Y_{abc}}{I_{x_a x_b}}.$$

We will need several limits of the expressions for Y and X , namely when pairs of distinct points collapse into each other

$$Y_{113} \equiv \lim_{x_2 \rightarrow x_1} Y_{123} = \left(2 - \log \left(\frac{\epsilon^2}{x_{13}^2} \right)\right) \frac{I_{x_1 x_3}}{16\pi^2},$$

$$X_{1134} \equiv \lim_{x_2 \rightarrow x_1} X_{1234} = \left(2 - \log \left(\frac{\epsilon^2 x_{34}^2}{x_{13}^2 x_{14}^2} \right)\right) \frac{I_{x_1 x_3} I_{x_1 x_4}}{16\pi^2},$$

where we are considering $x_2^\mu = x_1^\mu + \epsilon^\mu$ with $\epsilon^\mu \rightarrow 0$. We can also take a further limit of the last expression above when $x_4 \rightarrow x_3$ giving

$$X_{1133} = \left(1 - \log \left(\frac{\epsilon^2}{x_{13}^2} \right)\right) \frac{I_{x_1 x_3}^2}{8\pi^2}.$$

Moreover, we also need limits of the first and second derivatives of both the Y and the X integrals. We include the results of them below for completeness. The first derivatives are given by

$$\lim_{x_2 \rightarrow x_1} \partial_{1,\mu} Y_{123} = \frac{\epsilon_\mu}{\epsilon^2} \frac{I_{x_1 x_3}}{8\pi^2} - \left(1 - \log \left(\frac{\epsilon^2}{x_{13}^2} \right)\right) \frac{x_{13,\mu} I_{x_1 x_3}^2}{4} - \frac{x_{13,\nu} \epsilon^\nu \epsilon_\mu I_{x_1 x_3}^2}{2\epsilon^2}, \quad (\text{B.2})$$

$$\lim_{x_2 \rightarrow x_1} \partial_{3,\mu} Y_{123} = \left(1 - \log \left(\frac{\epsilon^2}{x_{13}^2} \right)\right) \frac{x_{13,\mu} I_{x_1 x_3}^2}{2}, \quad (\text{B.3})$$

$$\lim_{x_2 \rightarrow x_1} \partial_{1,\mu} X_{1234} = \frac{\epsilon_\mu}{\epsilon^2} \frac{I_{x_1 x_3} I_{x_1 x_4}}{8\pi^2} - \left(1 - \log \left(\frac{\epsilon^2 x_{34}^2}{x_{13}^2 x_{14}^2} \right)\right) \frac{x_{13,\mu} I_{x_1 x_3}^2 I_{x_1 x_4} + x_{14,\mu} I_{x_1 x_3} I_{x_1 x_4}^2}{4}$$

$$- \frac{x_{14,\nu} \epsilon^\nu \epsilon_\mu I_{x_1 x_3} I_{x_1 x_4}^2}{2\epsilon^2} - \frac{x_{13,\nu} \epsilon^\nu \epsilon_\mu I_{x_1 x_3}^2 I_{x_1 x_4}}{2\epsilon^2},$$

$$\lim_{x_2 \rightarrow x_1} \partial_{3,\mu} X_{1234} = -\frac{x_{34,\mu} I_{x_1 x_3} I_{x_1 x_4} I_{x_3 x_4}}{2} + \left(1 - \log \left(\frac{\epsilon^2 x_{34}^2}{x_{13}^2 x_{14}^2} \right)\right) \frac{x_{13,\mu} I_{x_1 x_3}^2 I_{x_1 x_4}}{2},$$

As before, one can take further limits of these expressions when needed. The second derivatives read

$$\lim_{x_2 \rightarrow x_1} \partial_{1,\mu} \partial_{2,\nu} Y_{123} = -\frac{\epsilon_\mu \epsilon_\nu}{\epsilon^4} \frac{I_{x_1 x_3}}{4\pi^2} + \frac{\epsilon_\mu \epsilon_\nu I_{x_1 x_3}^2}{\epsilon^2} \left(\frac{1}{6} + \frac{x_{13,\rho} \epsilon^\rho}{\epsilon^2} - \frac{16\pi^2 x_{13,\rho} \epsilon^\rho x_{13,\sigma} \epsilon^\sigma I_{x_1 x_3}}{3\epsilon^2} \right)$$

$$+ \frac{\epsilon_\nu}{\epsilon^2} \frac{x_{13,\mu} I_{x_1 x_3}^2}{2} - \frac{\epsilon_\mu}{\epsilon^2} \frac{x_{13,\nu} I_{x_1 x_3}^2}{2} + \frac{8\pi^2 x_{13,\rho} \epsilon^\rho I_{x_1 x_3}^3}{3\epsilon^2} (2x_{13,\nu} \epsilon_\mu - x_{13,\mu} \epsilon_\nu)$$

$$+ \frac{1}{\epsilon^2} \frac{\delta_{\mu\nu} I_{x_1 x_3}}{8\pi^2} - \delta_{\mu\nu} I_{x_1 x_3}^2 \left(\frac{11}{36} + \frac{x_{13,\rho} \epsilon^\rho}{2\epsilon^2} - \frac{8\pi^2 x_{13,\rho} \epsilon^\rho x_{13,\sigma} \epsilon^\sigma I_{x_1 x_3}}{3\epsilon^2} \right)$$

$$+ \frac{1}{12} \log \left(\frac{\epsilon^2}{x_{13}^2} \right) I_{x_1 x_3}^2 \delta_{\mu\nu} + \frac{2\pi^2}{9} \left(1 - 6 \log \left(\frac{\epsilon^2}{x_{13}^2} \right) \right) x_{13,\mu} x_{13,\nu} I_{x_1 x_3}^3,$$

$$\begin{aligned} \lim_{x_2 \rightarrow x_1} \partial_{1,\mu} \partial_{3,\nu} Y_{123} &= \frac{\epsilon_\mu \epsilon_\nu}{\epsilon^2} \frac{I_{x_1 x_3}^2}{2} + \frac{\epsilon_\mu}{\epsilon^2} x_{13,\nu} I_{x_1 x_3}^2 - 2\pi^2 \left(1 - 2 \log \left(\frac{\epsilon^2}{x_{13}^2} \right) \right) x_{13,\mu} x_{13,\nu} I_{x_1 x_3}^3 \\ &+ \frac{1}{4} \left(1 - \log \left(\frac{\epsilon^2}{x_{13}^2} \right) \right) I_{x_1 x_3}^2 \delta_{\mu\nu} - \frac{8\pi^2 x_{13,\nu} \epsilon_\mu x_{13,\rho} \epsilon^\rho I_{x_1 x_3}^3}{\epsilon^2}, \end{aligned} \quad (\text{B.4})$$

$$\begin{aligned} \lim_{x_2 \rightarrow x_1} \partial_{1,\mu} \partial_{2,\nu} X_{1234} &= -\frac{\epsilon_\mu \epsilon_\nu}{\epsilon^4} \frac{I_{x_1 x_3} I_{x_1 x_4}}{4\pi^2} + \frac{\epsilon_\mu \epsilon_\nu I_{x_1 x_3}^2 I_{x_1 x_4}^2}{6\epsilon^2} \left(\frac{1}{I_{x_3 x_4}} - \frac{32\pi^2 x_{13,\rho} \epsilon^\rho x_{14,\sigma} \epsilon^\sigma}{\epsilon^2} \right) \\ &+ \frac{\epsilon_\mu \epsilon_\nu \epsilon^\rho I_{x_1 x_3} I_{x_1 x_4}}{\epsilon^4} (x_{14,\rho} I_{x_1 x_4} + x_{13,\rho} I_{x_1 x_3}) \\ &- \frac{16\pi^2 \epsilon_\mu \epsilon_\nu \epsilon^\rho \epsilon^\sigma I_{x_1 x_3} I_{x_1 x_4}}{3\epsilon^4} (x_{14,\rho} x_{14,\sigma} I_{x_1 x_4}^2 + x_{13,\rho} x_{13,\sigma} I_{x_1 x_3}^2) \\ &- \frac{\epsilon_\mu I_{x_1 x_3} I_{x_1 x_4}}{2\epsilon^2} (x_{14,\nu} I_{x_1 x_4} + x_{13,\nu} I_{x_1 x_3}) \\ &+ \frac{\epsilon_\nu I_{x_1 x_3} I_{x_1 x_4}}{2\epsilon^2} (x_{14,\mu} I_{x_1 x_4} + x_{13,\mu} I_{x_1 x_3}) \\ &+ \frac{8\pi^2 \epsilon_\mu \epsilon^\rho I_{x_1 x_3} I_{x_1 x_4}}{3\epsilon^2} (2x_{14,\nu} x_{14,\rho} I_{x_1 x_4}^2 + x_{13,\rho} x_{14,\nu} I_{x_1 x_3} I_{x_1 x_4}) \\ &+ \frac{8\pi^2 \epsilon_\mu \epsilon^\rho I_{x_1 x_3} I_{x_1 x_4}}{3\epsilon^2} (2x_{13,\nu} x_{13,\rho} I_{x_1 x_3}^2 + x_{14,\rho} x_{13,\nu} I_{x_1 x_3} I_{x_1 x_4}) \\ &- \frac{4\pi^2 \epsilon_\nu \epsilon^\rho I_{x_1 x_3} I_{x_1 x_4}}{3\epsilon^2} (2x_{14,\mu} x_{14,\rho} I_{x_1 x_4}^2 + x_{13,\rho} x_{14,\mu} I_{x_1 x_3} I_{x_1 x_4}) \\ &- \frac{4\pi^2 \epsilon_\nu \epsilon^\rho I_{x_1 x_3} I_{x_1 x_4}}{3\epsilon^2} (2x_{13,\mu} x_{13,\rho} I_{x_1 x_3}^2 + x_{14,\rho} x_{13,\mu} I_{x_1 x_3} I_{x_1 x_4}) \\ &+ \frac{1}{\epsilon^2} \frac{I_{x_1 x_3} I_{x_1 x_4} \delta_{\mu\nu}}{8\pi^2} - \frac{I_{x_1 x_3} I_{x_1 x_4} \delta_{\mu\nu}}{4} (I_{x_1 x_4} + I_{x_1 x_3}) \\ &- \frac{I_{x_1 x_3} I_{x_1 x_4} \delta_{\mu\nu} \epsilon^\rho}{2\epsilon^2} (x_{14,\rho} I_{x_1 x_4} + x_{13,\rho} I_{x_1 x_3}) \\ &+ \frac{8\pi^2 I_{x_1 x_3} I_{x_1 x_4} \delta_{\mu\nu} \epsilon^\rho \epsilon^\sigma}{3\epsilon^2} (x_{14,\rho} x_{14,\sigma} I_{x_1 x_4}^2 + x_{13,\rho} x_{13,\sigma} I_{x_1 x_3}^2) \\ &+ \frac{8\pi^2 I_{x_1 x_3} I_{x_1 x_4} \delta_{\mu\nu} \epsilon^\rho \epsilon^\sigma}{3\epsilon^2} x_{13,\rho} x_{14,\sigma} I_{x_1 x_3} I_{x_1 x_4} \\ &+ \frac{1}{36} \left(-2 + 3 \log \left(\frac{\epsilon^2 x_{34}^2}{x_{13}^2 x_{14}^2} \right) \right) \frac{I_{x_1 x_3}^2 I_{x_1 x_4}^2 \delta_{\mu\nu}}{I_{x_3 x_4}} \\ &+ \frac{2\pi^2}{9} \left(1 - 6 \log \left(\frac{\epsilon^2 x_{34}^2}{x_{13}^2 x_{14}^2} \right) \right) x_{13,\mu} x_{13,\nu} I_{x_1 x_3}^3 I_{x_1 x_4} \\ &- \frac{2\pi^2}{9} \left(1 + 3 \log \left(\frac{\epsilon^2 x_{34}^2}{x_{13}^2 x_{14}^2} \right) \right) (x_{13,\nu} x_{14,\mu} + x_{13,\mu} x_{14,\nu}) I_{x_1 x_3}^2 I_{x_1 x_4}^2 \\ &+ \frac{2\pi^2}{9} \left(1 - 6 \log \left(\frac{\epsilon^2 x_{34}^2}{x_{13}^2 x_{14}^2} \right) \right) x_{14,\mu} x_{14,\nu} I_{x_1 x_3} I_{x_1 x_4}^3, \\ \lim_{x_2 \rightarrow x_1} \partial_{1,\mu} \partial_{3,\nu} X_{1234} &= \frac{\epsilon_\mu \epsilon_\nu}{\epsilon^2} \frac{I_{x_1 x_3}^2 I_{x_1 x_4}}{2} + 2\pi^2 \log \left(\frac{\epsilon^2 x_{34}^2}{x_{13}^2 x_{14}^2} \right) x_{13,\nu} x_{14,\mu} I_{x_1 x_3}^2 I_{x_1 x_4}^2 \\ &+ \frac{x_{13,\nu} \epsilon_\mu I_{x_1 x_3}^2 I_{x_1 x_4}}{\epsilon^2} (1 - 4\pi^2 x_{14,\rho} \epsilon^\rho I_{x_1 x_4} - 8\pi^2 x_{13,\rho} \epsilon^\rho I_{x_1 x_3}) \end{aligned}$$

$$\begin{aligned}
& + 2\pi^2 \left(-1 + 2 \log \left(\frac{\epsilon^2 x_{34}^2}{x_{13}^2 x_{14}^2} \right) \right) x_{13,\mu} x_{13,\nu} I_{x_1 x_3}^3 I_{x_1 x_4} \\
& - \frac{1}{4} \left(-1 + \log \left(\frac{\epsilon^2 x_{34}^2}{x_{13}^2 x_{14}^2} \right) \right) I_{x_1 x_3}^2 I_{x_1 x_4} \delta_{\mu,\nu} \\
& + 2\pi^2 x_{13,\mu} x_{34,\nu} I_{x_1 x_3}^2 I_{x_1 x_4} I_{x_3 x_4} + 2\pi^2 x_{14,\mu} x_{34,\nu} I_{x_1 x_3} I_{x_1 x_4}^2 I_{x_3 x_4} ,
\end{aligned}$$

$$\begin{aligned}
\lim_{x_2 \rightarrow x_1} \partial_{3,\mu} \partial_{4,\nu} X_{1234} &= \frac{\delta_{\mu\nu}}{2} I_{x_1 x_3} I_{x_1 x_4} I_{x_3 x_4} - 4\pi^2 x_{34,\mu} x_{34,\nu} I_{x_1 x_3} I_{x_1 x_4} I_{x_3 x_4}^2 \\
& - 4\pi^2 x_{14,\nu} x_{34,\mu} I_{x_1 x_3} I_{x_1 x_4}^2 I_{x_3 x_4} + 4\pi^2 x_{13,\mu} x_{34,\nu} I_{x_1 x_3}^2 I_{x_1 x_4} I_{x_3 x_4} \\
& - 4\pi^2 x_{13,\mu} x_{14,\nu} \log \left(\frac{\epsilon^2 x_{34}^2}{x_{13}^2 x_{14}^2} \right) I_{x_1 x_3}^2 I_{x_1 x_4}^2 .
\end{aligned}$$

Using the above results, we can proceed to the computation of the two- and three-point functions. The result of all the non-zero Feynman diagrams relevant for us is given in figure 5, where we have omitted terms involving $\epsilon^{\mu\nu\rho\lambda}$ that must either vanish when a pair of point collide or cancel when all the diagrams are summed. This is the case in order to preserve conformal invariance and parity.

The results of figure 5 only contain derivatives of the function $H_{12,34}$ and it is possible to evaluate them explicitly [33]. Consider the case when the derivatives act on either the first or the second pair of points of H , namely $\partial_1 \cdot \partial_2 H_{12,34}$, and also the case when they act on a point belonging to the first pair and a point belonging to the second pair, for instance $\partial_1 \cdot \partial_4 H_{12,34}$. The first case is straightforward to compute by using integration by parts and the property of the euclidean propagator $\square_x I_{xy} = -\delta^{(4)}(x-y)$. The result is

$$\partial_1 \cdot \partial_2 H_{12,34} = \frac{1}{2} (Y_{134} I_{x_1 x_2} + Y_{234} I_{x_1 x_2} - X_{1234}) . \quad (\text{B.5})$$

For computing the second case, we need the function $F_{12,34}$ defined in (B.1) and some identities of $H_{12,34}$. Firstly, note that H satisfies the equation

$$(\partial_{1,\mu} + \partial_{2,\mu} + \partial_{3,\mu} + \partial_{4,\mu}) H_{12,34} = 0 , \quad (\text{B.6})$$

which can be proved by integration by parts. Similarly, it is possible to show that the following identity holds

$$\partial_i \cdot \partial_j H_{12,34} = \frac{1}{2} (\square_k + \square_l - \square_i - \square_j) H_{12,34} + \partial_k \cdot \partial_l H_{12,34} \quad (\text{B.7})$$

for $i \neq j \neq k \neq l$. In order to get $\partial_1 \cdot \partial_4 H_{12,34}$, it is convenient to write it as

$$\partial_1 \cdot \partial_4 H_{12,34} = \frac{1}{2} (\partial_1 \cdot \partial_3 + \partial_1 \cdot \partial_4) H_{12,34} - \frac{1}{2} (\partial_1 \cdot \partial_3 - \partial_1 \cdot \partial_4) H_{12,34} . \quad (\text{B.8})$$

Now using (B.7), one can show that the first term on the right-hand side of (B.8) can be written as

$$\frac{1}{2} (\partial_1 \cdot \partial_3 + \partial_1 \cdot \partial_4) H_{12,34} = -\frac{1}{2} (\square_1 H_{12,34} + \partial_1 \cdot \partial_2 H_{12,34}) \quad (\text{B.9})$$

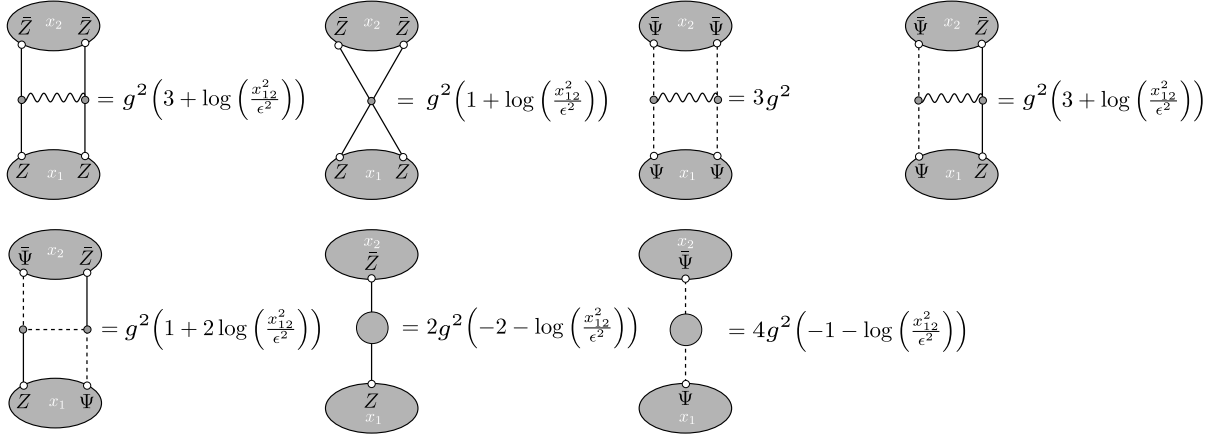


Figure 6: The results of the Feynman diagrams for the two-point functions. They are obtained by taking the limits $x_3 \rightarrow x_2$ and $x_4 \rightarrow x_1$ of the expressions in figure 5.

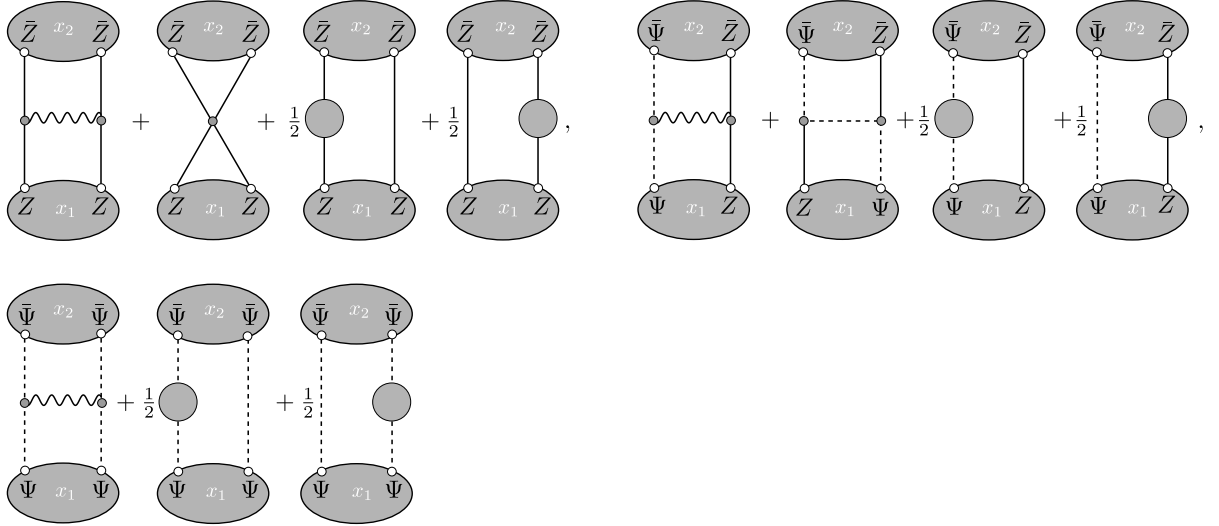


Figure 7: Using the results of figure 6, the sum of the graphs appearing in this figure gives precisely the $\mathfrak{su}(1|1)$ Hamiltonian of (B.11).

where $\square_i H_{12,34}$ can be computed using the equation defining the euclidean propagator and $\partial_1 \cdot \partial_2 H_{12,34}$ is known from (B.5). Using (B.6), the second term on the right-hand side of (B.8) can be written as

$$\frac{1}{2} (\partial_1 \cdot \partial_3 - \partial_1 \cdot \partial_4) H_{12,34} = \frac{1}{4} (F_{12,34} I_{x_1 x_2} I_{x_3 x_4} + (\square_4 - \square_3) H_{12,34}) . \quad (\text{B.10})$$

Finally, substituting (B.9) and (B.10) in (B.8), one gets an expression for $\partial_1 \cdot \partial_4 H_{12,34}$. The expressions for the remaining cases where the derivatives act on other points can be deduced analogously.

In order to get the two-point functions, one takes the limit where two pairs of points collapse into each other that is $x_4 \rightarrow x_1$ and $x_3 \rightarrow x_2$. The results of these limits are given in figure 6. Summing all the diagrams as illustrated in figure 7, one obtains the one-loop Hamiltonian operator

$$H = 2g^2(I - SP), \quad (\text{B.11})$$

where SP is the superpermutator which exchanges the fields and picks up a minus sign when both fields are fermionic. This Hamiltonian is the well known result of [17, 13].

We now proceed to the three-point functions. In order to obtain the constant coming from each diagram, one takes the limit of the expressions given in figure 5 where a single pair of points collapses into each other. After taking that limit, the result will have constant terms, divergent logarithmic terms and eventually Y functions and their derivatives. The derivatives of the Y functions can be expressed in terms of the Y function itself by using some of its properties. This will be explained in detail in the Appendix C. After this procedure, the logarithmic terms will contribute to the standard regulator dependence in (3.8) and the remaining Y functions will cancel with similar contributions from other diagrams in a way that the conformal invariance is restored. One can then read the constant part of the diagram. The final step is to subtract one half the constant coming from the same diagram but when the two pairs of points collapse into each other as described in figure 3. The results are given in figure 4.

Let us comment now on a detail of this computation. Our final results presented in the figures 4 and 5 do not contain the Feynman diagrams of figure 8. This is the case because the first two graphs of this figure turn out to cancel among them. They can give a non-zero contribution in our setup only when either $b = c = 4$ and $a = 3$ or $a = c = 2$ and $b = 3$. However, as these two graphs always appear with the same weight and opposite signs, they end up canceling. The last graph of the figure 8 must vanish when $|x_{12}| \rightarrow 0$ because it is

$$\propto \epsilon^{\gamma\delta} \epsilon^{\dot{\gamma}\dot{\delta}} \sigma_{E\dot{\gamma}\dot{\delta}}^\mu \sigma_{E\dot{\delta}\dot{\gamma}}^\nu \sigma_{E\dot{\gamma}\dot{\delta}}^\rho \sigma_{E\dot{\delta}\dot{\gamma}}^\lambda \int d^4v d^4u (\partial_\mu^v I_{x_1v}) (\partial_\nu^v I_{x_2v}) I_{vu} (\partial_\rho^u I_{x_3u}) (\partial_\lambda^u I_{x_4u}) \rightarrow 0.$$

If it was non-vanishing it would produce a term with a different tensor structure of (3.8) which would violate conformal invariance.

C Some examples of three-point functions

In this Appendix, we give two examples of three-point functions. The first one is the case of three half-BPS operators. It is well-known that this correlator is protected and therefore it constitutes a check for our computations. Then we compute a non-protected three-point function both by brute force and by using our prescription of inserting the operator \mathcal{F} at the splitting points.

C.1 Three half-BPS operators

Consider the following three half-BPS operators

$$\mathcal{O}_1 = \text{Tr}(ZZ), \quad (\text{C.1})$$

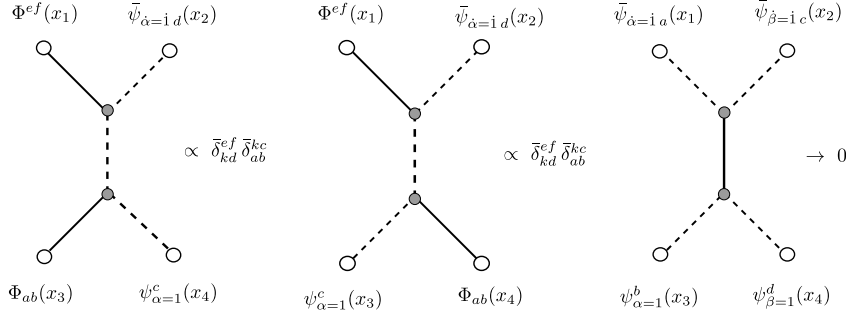


Figure 8: The additional Feynman diagrams that do not contribute in the setup considered in this work. The solid and dashed lines represent the scalars and fermions, respectively.

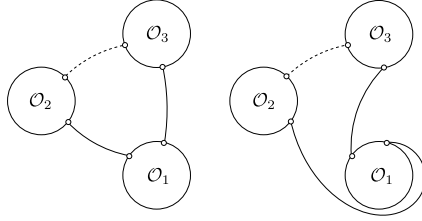


Figure 9: The tree-level diagrams for the three-point functions of the three half-BPS operators considered in (C.1)-(C.3). Note that only the first term of \mathcal{O}_3 in (C.3) gives a non-zero contribution at this order in perturbation theory as the second term clearly gives a vanishing contribution due to R -charge conservation.

$$\mathcal{O}_2 = \text{Tr}(\bar{\Psi}\bar{Z}) \ , \quad (\text{C.2})$$

$$\mathcal{O}_3 = (\mathfrak{R}_4^2 \mathfrak{R}_3^1) \cdot \text{Tr}(\Psi Z) = \text{Tr}(\Psi\bar{Z}) + \text{Tr}(\psi^2 \Phi^{14}) \ . \quad (\text{C.3})$$

At tree-level the result is simply given by the sum of the two diagrams of figure 9 and reads

$$\langle \mathcal{O}_1(x_1) \mathcal{O}_2(x_2) \mathcal{O}_3(x_3) \rangle = \frac{2}{(2\pi)^6 8^2 x_{12}^2 x_{13}^2} (\sigma_E^\mu)_{1\dot{1}} \partial_{3,\mu} \frac{1}{2x_{23}^2} \ . \quad (\text{C.4})$$

At one-loop, one has to sum the diagrams of figure 10 and use the results given in figure 5 taking the appropriate limits. Some diagrams will still contain the function Y and its first derivatives. The Y function depends on the external points in a way that does not respect the spacetime dependence fixed by conformal symmetry, see equation (3.8). However, when one sums the different diagrams this non-conformal spacetime dependence turns out to cancel identically.

At the end of the day, summing all the diagrams gives a vanishing one-loop contribution to the structure constant in agreement with the non-renormalization theorem for the three-points functions of half-BPS operators introduced in [19]. Equivalently, one can also use our prescription to reproduce this one-loop result. One simply has to sum over the insertions represented in figure 11 obtaining zero as expected.

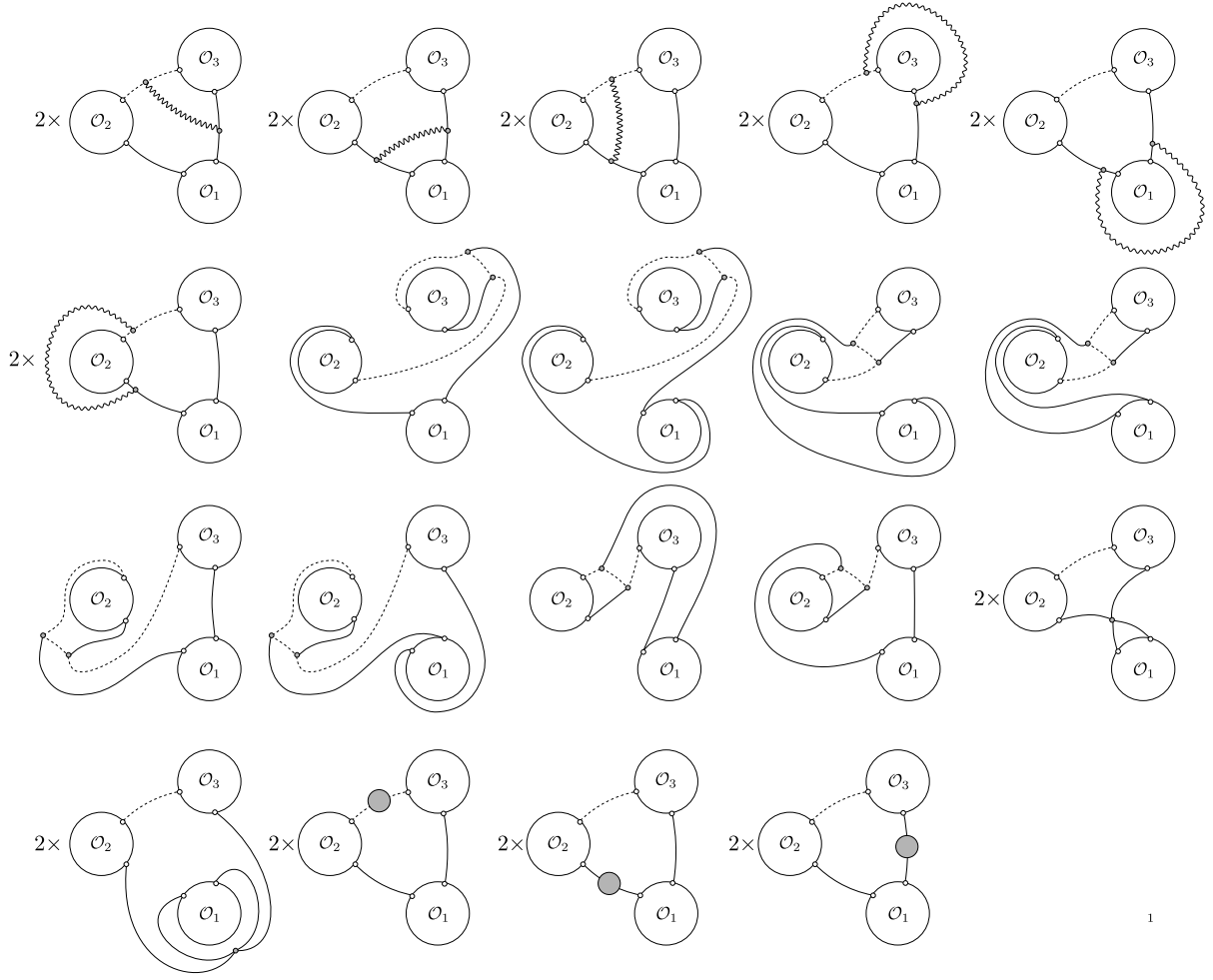


Figure 10: The one-loop diagrams contributing to the three-point function of the three half-BPS operators considered in (C.1)-(C.3). In the last four diagrams of the second row, the second term of \mathcal{O}_3 (see expression (C.3)) gives a non-zero result. In all other diagrams only the first term of \mathcal{O}_3 contributes.

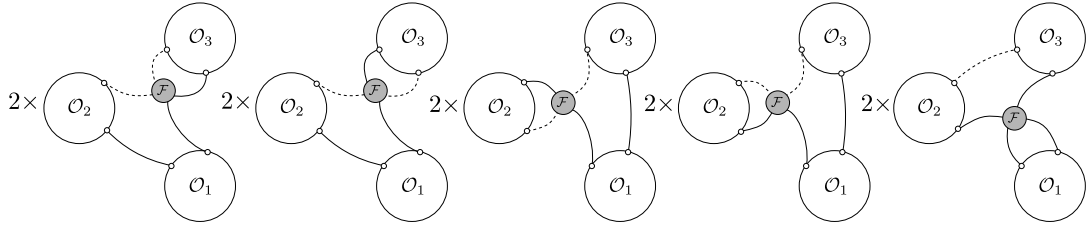


Figure 11: Inserting the \mathcal{F} operator at the splitting points, one reproduces the vanishing result expected for a three-point function of half-BPS operators. Apart from the graphics in the figure, there are similar graphics with the operator \mathcal{F} acting in the remaining splitting points.

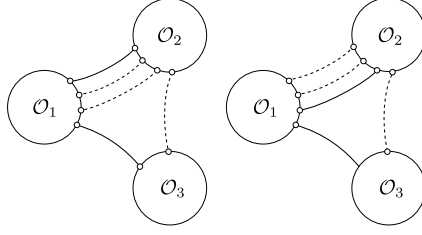


Figure 12: The tree-level diagrams contributing to the three-point function of the operators (C.5)-(C.7). Once again, we only need to consider the first term of (C.7) at this order in perturbation theory.

C.2 Two non-BPS and one half-BPS operators

We consider now a non-protected three-point function. This example serves as an illustration of some of the technical details of the brute force computation. Moreover, we also use it to check our prescription of the \mathcal{F} operator insertion at the splitting points. The operators at one-loop level that we will consider are

$$\mathcal{O}_1 = \text{Tr} (Z\Psi\Psi Z) , \quad (\text{C.5})$$

$$\mathcal{O}_2 = \text{Tr} (\bar{Z}\bar{\Psi}\bar{\Psi}\bar{Z}) , \quad (\text{C.6})$$

$$\mathcal{O}_3 = (\mathfrak{R}^2_4 \mathfrak{R}^1_3) \cdot \text{Tr} (\Psi Z) = \text{Tr} (\Psi \bar{Z}) + \text{Tr} (\psi^2 \Phi^{14}) . \quad (\text{C.7})$$

Note that the \mathcal{O}_1 and \mathcal{O}_2 are not half-BPS and therefore they will receive corrections as explained in section 3.1. However, to compute the Feynman diagrams contribution we do not need to take them into account. At tree-level the result is simply the sum of the two diagrams of figure 12 which gives

$$\begin{aligned} \langle \mathcal{O}_1(x_1) \mathcal{O}_2(x_2) \mathcal{O}_3(x_3) \rangle_0 &= -\frac{2}{(2\pi)^{10} 8^2 x_{13}^2 x_{12}^2} \\ &\times \left((\sigma_E^\mu)_{1i} \partial_{1,\mu} \frac{1}{2x_{12}^2} \right) \left((\sigma_E^\nu)_{1i} \partial_{1,\nu} \frac{1}{2x_{12}^2} \right) \left((\sigma_E^\rho)_{1i} \partial_{3,\rho} \frac{1}{2x_{23}^2} \right) . \end{aligned}$$

The diagrams contributing at one-loop are represented in figure 13.

As in the previous example, the dependence of each diagram on the Y function and its derivatives will cancel when we sum over all the diagrams. This ensures that we obtain a conformal invariant result. However, this cancellation is not immediate and it relies on several properties of the Y function. The first observation is that the function Y is given by

$$Y_{123} = \frac{\pi^2 \phi(r, s)}{(2\pi)^4} I_{x_1, x_3} , \quad (\text{C.8})$$

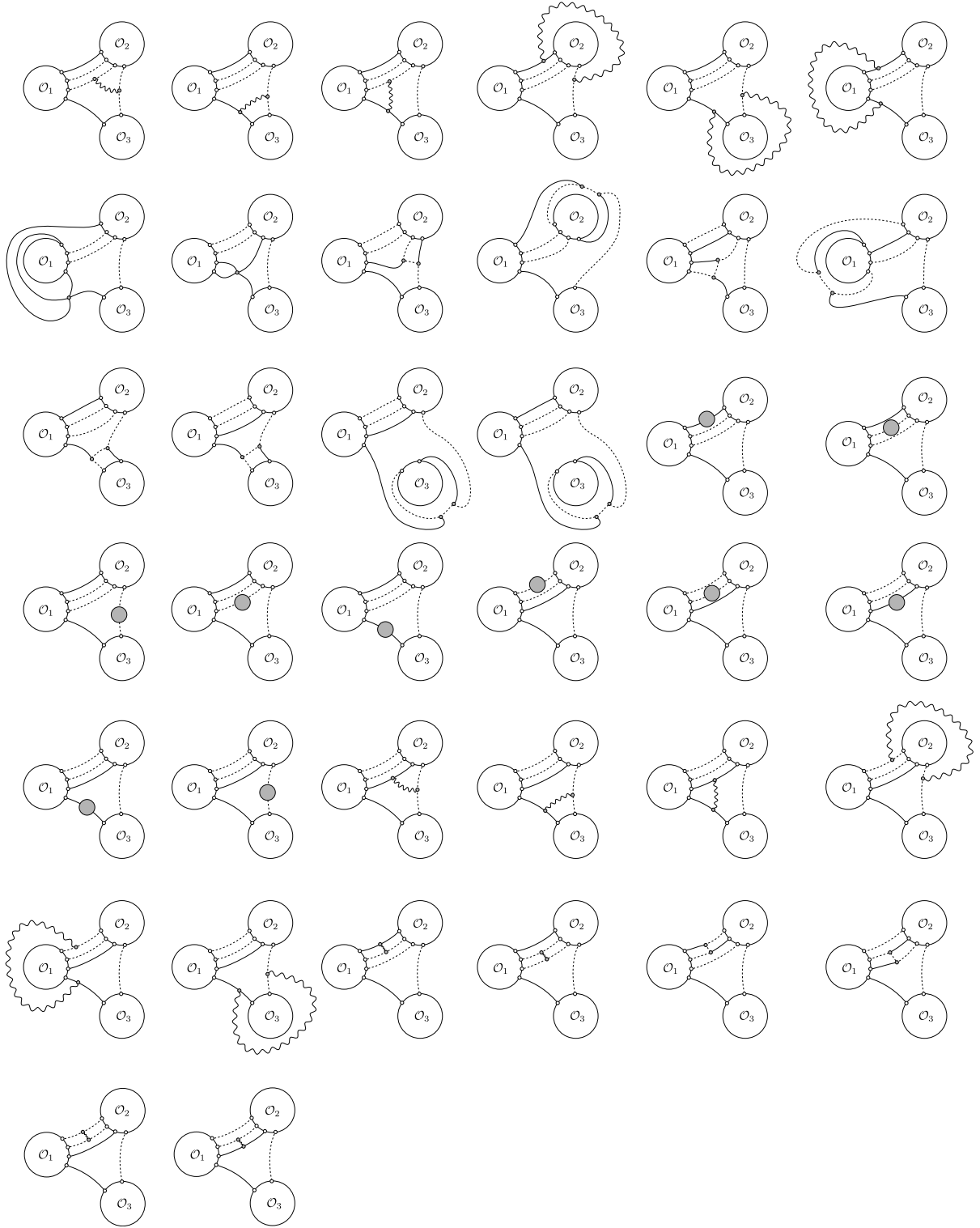


Figure 13: The relevant one-loop diagrams for the three-point function of the operators (C.5)-(C.7). The second term of (C.7) gives a non-zero contribution namely the first four diagrams of the third row.

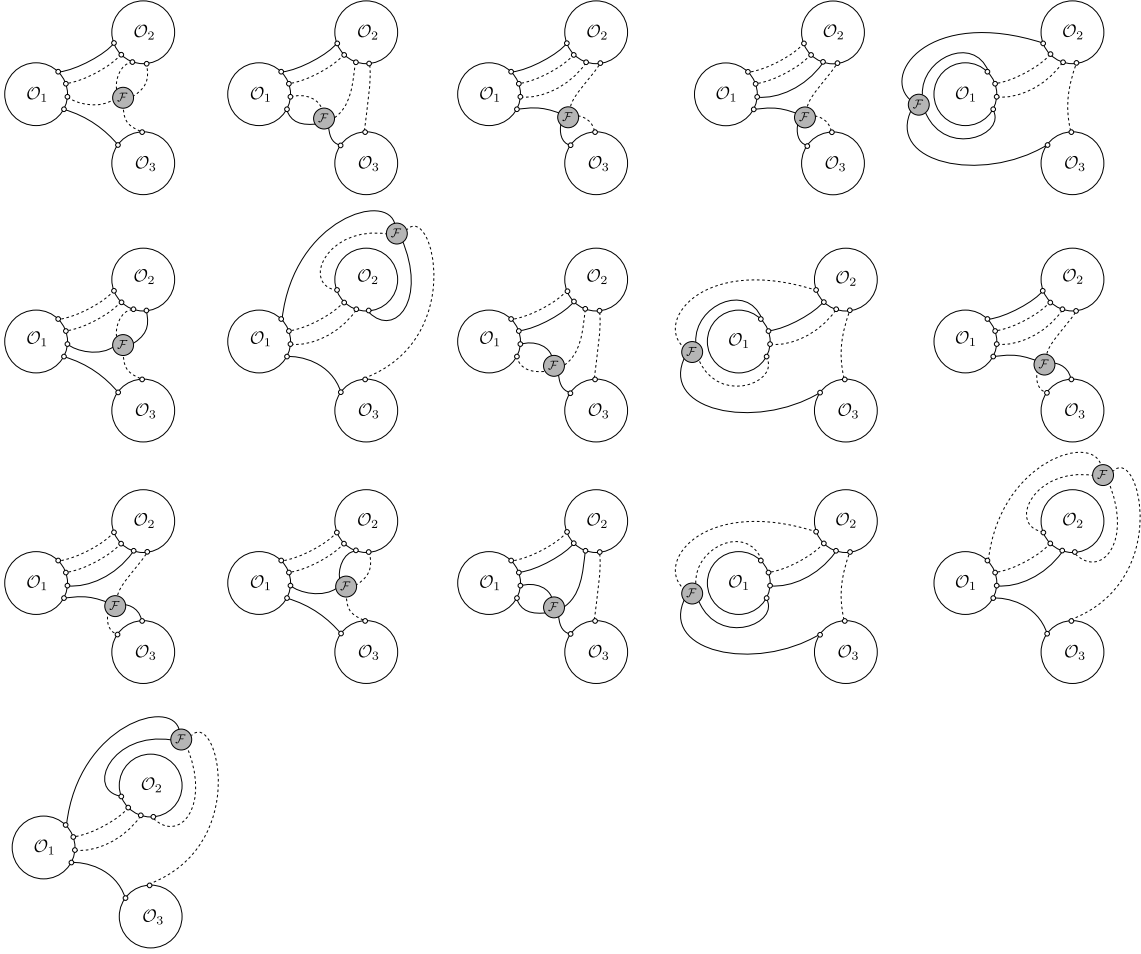


Figure 14: Inserting the operator \mathcal{F} at the splitting points reproduce the result of the one-loop Feynman diagrams.

where $r = \frac{x_{12}^2}{x_{13}^2}$ and $s = \frac{x_{23}^2}{x_{13}^2}$ and an explicit expression for $\phi(r, s)$ can be found in [32]. The important information for us is that the function ϕ satisfies the following differential equations [7]

$$\begin{aligned} \phi(r, s) + (s + r - 1)\partial_s \phi(r, s) + 2r\partial_r \phi(r, s) &= -\frac{\log r}{s}, \\ \phi(r, s) + (s + r - 1)\partial_r \phi(r, s) + 2s\partial_s \phi(r, s) &= -\frac{\log s}{r}, \end{aligned} \quad (\text{C.9})$$

which can be used to relate the first derivatives of Y with Y itself. In addition, one can take derivatives with respect to r and s of both the equations above to arrive at a system of equations that relates second derivatives of ϕ with first derivatives and the function ϕ itself. Using then (C.8), it is trivial to get rid of the second derivatives of Y . These properties of the function ϕ ensure that the non-conformal dependence of the three-point function indeed cancel when all diagrams are summed over.

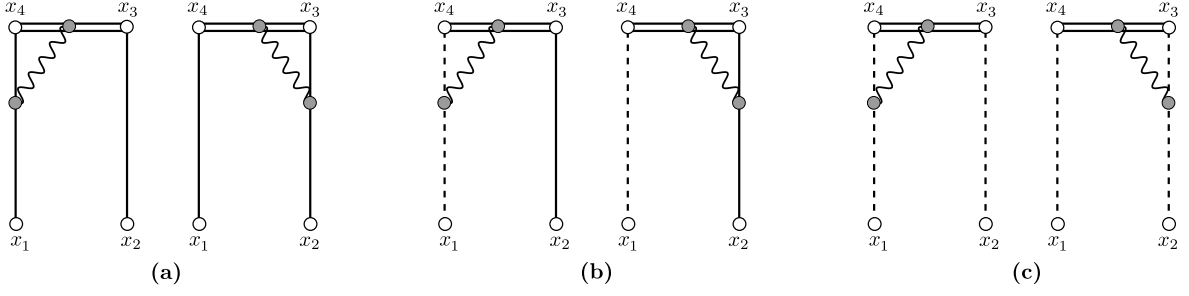


Figure 15: The one-loop additional graphs coming from the Wilson line.

The final result is given by

$$\langle \mathcal{O}_1(x_1) \mathcal{O}_2(x_2) \mathcal{O}_3(x_3) \rangle = \langle \mathcal{O}_1 \mathcal{O}_2 \mathcal{O}_3 \rangle_0 \left(1 + 4g^2 \left(-1 + 2 \log \left(\frac{\epsilon^2}{x_{12}^2} \right) \right) + \mathcal{O}(g^4) \right)$$

which comparing with (3.8) gives the correct anomalous dimensions of the operators. This is a non-trivial consistency check of our computation.

The structure constant can now be obtained by also computing the constants from the two-point functions. We have all the tools at hand to perform such calculation and read the one-loop constant. We obtain the following contribution from the Feynman diagrams to the structure constant

$$C_{123}^{(1)} \Big|_{\text{Feynman diagrams contribution}} = -\frac{3}{2}. \quad (\text{C.10})$$

Recall that this is not the final result, one also has to add the extra contribution from the corrected two-loop Bethe states.

Finally, it is possible to test our prescription of inserting the \mathcal{F} operator at the splitting points, see figure 14. Summing over all these insertions gives precisely the contribution (C.10) to the structure constant.

D Wilson line contribution

As mentioned before, the point splitting regularization breaks explicitly the gauge invariance due to the fact that some fields inside the trace are now at a slightly different spacetime points. The introduction of a Wilson line connecting these fields restore the gauge invariance at the price of introducing extra Feynman diagrams. In this Appendix, we show that these extra diagrams do not contribute to the scheme and normalization independent structure constant $C_{123}^{(1)}$ defined in (3.8).

D.1 Wilson line connecting two scalars

In our conventions the Wilson line operator is defined by

$$W_l = \mathcal{P} \exp \left[i g_{YM} \int A_\mu d\vec{x}^\mu \right].$$

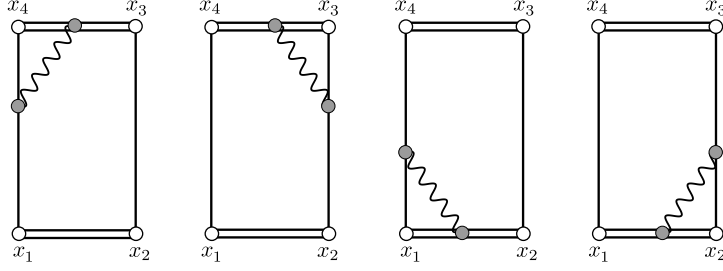


Figure 16: The Wilson line contributions to the two-point functions. In the combination of the two- and the three-point diagrams that provide the scheme independent structure constant (3.8), all the extra diagrams coming from the Wilson lines cancel each other at this order in perturbation theory. In the figure, the diagram corresponding to the emission of a gluon between the two Wilson lines is not depicted, since it is proportional to ϵ^2 and vanishes in the limit $\epsilon \rightarrow 0$.

When inserting a Wilson line connecting two scalars, it is necessary to consider the one-loop graphs corresponding to the gluon emission depicted in figure 15(a). Let us define $\epsilon^\mu = x_4^\mu - x_3^\mu$ and at the end of the day we will take the limit $\epsilon^\mu \rightarrow 0$. Then we can conveniently parametrize the Wilson line by $x^\mu(z) = x_3^\mu + z\epsilon^\mu$. The result of the sum of the diagrams is

$$\text{figure 15(a)} = \frac{\lambda}{128} \int_0^1 dz \epsilon_\mu (I_{x_2x_3} \partial_1^\mu Y_{1x_4} - I_{x_1x_4} \partial_2^\mu Y_{2x_3} + I_{x_1x_4} \partial_3^\mu Y_{2x_3} - I_{x_2x_3} \partial_4^\mu Y_{1x_4}) , \quad (\text{D.1})$$

where we have suppressed both the R -charge and the gauge indices which are the same as in the tree-level case. From the formula (B.3), it follows that the first and second terms of the above result are of order ϵ and therefore vanish in the limit $\epsilon \rightarrow 0$. However, from (B.2) we see that the third and last term give a finite contribution.

In order to compute the scheme and normalization structure constant $C_{123}^{(1)}$ of (3.8), we have to subtract from the previous result one half of the one-loop diagrams from the two-point functions as shown in figure 16 (we take both the limits $x_4 \rightarrow x_3$ and $x_2 \rightarrow x_1$). It is simple to show that the contribution of these diagrams cancels exactly the constant coming from the expression (D.1). So, at this order in perturbation theory we do not get any further contribution to $C_{123}^{(1)}$ and therefore we can safely ignore the Wilson lines.

D.2 Wilson line connecting either a scalar and a fermion or two fermions

In the case of a scalar and a fermion connected by a Wilson line, the contribution of the diagrams depicted in 15(b) is given by

$$\begin{aligned} \text{figure 15(b)} = \frac{\lambda}{32} \int_0^1 dz \epsilon^\mu \Big[& I_{x_2x_3} (\sigma_{E\mu 1i} \partial^4 \cdot \partial^1 Y_{1x_4} - \sigma_{E1i}^\nu \partial_\nu^4 \partial_\mu^1 Y_{1x_4} - \sigma_{E1i}^\nu \partial_\mu^4 \partial_\nu^1 Y_{1x_4} \\ & - \epsilon_{\rho\mu\lambda\nu} \sigma_{E1i}^\nu \partial^{4,\lambda} \partial^{1,\rho} Y_{1x_4}) + \sigma_{E1i}^\nu \partial_\nu^1 I_{x_1x_4} (\partial_\mu^3 Y_{2x_3} - \partial_\mu^2 Y_{2x_3}) \Big] . \end{aligned} \quad (\text{D.2})$$

Using the expressions (B.2-B.4), one can easily see that this gives a finite contribution in the limit when ϵ goes to zero (in particular, the term with $\epsilon_{\rho\mu\lambda\nu}$ vanishes). To this result, we have again to subtract one half of the one-loop diagrams from the two-point functions as was done in the previous subsection for the case of two scalars. Once again, the contribution of these diagrams cancels exactly the expression (D.2).

In the case when we have a Wilson line connecting two fermions, the same argument holds. Hence at one-loop level, we can ignore the Wilson lines contributions in all cases.

E A note on the $\mathfrak{su}(1|1)$ invariance of the final result

In this Appendix, we address the question of the $\mathfrak{su}(1|1)$ invariance of our formula for the structure constant. In particular, this serves as a consistency check for the one-loop prescription we have computed.

Let us start by checking the tree-level structure constant. Its expression is given in (3.10) when $g \rightarrow 0$. One possible way of implementing a symmetry transformation on a state at any value of the coupling is to add a Bethe root with zero-momentum. It is clear from the Bethe equations that we obtain a state with the same energy and therefore belonging to the same multiplet as the original one. Consider then the states $|\mathbf{1}\rangle$ and $|\mathbf{2}\rangle$ with one of their momenta $p_j^{(1)}$ and $p_i^{(2)}$ being equal to zero. In this particular case, we can write apart from possible signs

$$|\mathbf{2}\rangle = \bar{\mathfrak{Q}} |\mathbf{2}, \{\hat{p}_i^{(2)}\}\rangle, \quad \langle \mathbf{1}^f | = \langle \mathbf{1}^f, \{\hat{p}_j^{(1)}\} | \bar{\mathfrak{S}},$$

where the hat over a p means that this momentum is absent. The operator $\bar{\mathfrak{Q}}$ ($\bar{\mathfrak{S}}$) creates (annihilates) a zero-momentum magnon on a ket and annihilates (creates) a zero-momentum magnon on the bra (we are omitting the R -charge and Lorentz indices for simplicity).

For this particular choice of momenta the expression (3.10) for $g = 0$ becomes

$$\langle \mathbf{1}^f, \{\hat{p}_j^{(1)}\} | \bar{\mathfrak{S}} \tilde{\mathcal{O}}_3 \bar{\mathfrak{Q}} |\mathbf{2}, \{\hat{p}_i^{(2)}\}\rangle = \langle \mathbf{1}^f, \{\hat{p}_j^{(1)}\} | \tilde{\mathcal{O}}_3 \{\bar{\mathfrak{S}}, \bar{\mathfrak{Q}}\} |\mathbf{2}, \{\hat{p}_i^{(2)}\}\rangle, \quad (\text{E.1})$$

where we denote the operator $|\bar{Z} \dots \bar{Z} i_1 \dots i_{L_2-N_3}\rangle \langle \bar{\Psi} \dots \bar{\Psi} i_1 \dots i_{L_2-N_3}|$ by $\tilde{\mathcal{O}}_3$. Moreover in this equality, we have used that $\bar{\mathfrak{S}}$ and $\tilde{\mathcal{O}}_3$ commute which can be proved by applying the commutator to a generic $\mathfrak{su}(1|1)$ state. In addition, we have also used that

$$\bar{\mathfrak{S}} |\mathbf{2}, \{\hat{p}_i^{(2)}\}\rangle = 0, \quad (\text{E.2})$$

as the state is primary.

Now, the anticommutator $\{\bar{\mathfrak{S}}, \bar{\mathfrak{Q}}\}$ is given by (see for instance the Appendix D of [34])

$$\{\bar{\mathfrak{S}}, \bar{\mathfrak{Q}}\} = \mathcal{L} + \frac{1}{2}H(g), \quad (\text{E.3})$$

where \mathcal{L} is the length operator and $H(g)$ is the dilatation operator. When acting on the state $|\mathbf{2}, \{\hat{p}_i^{(2)}\}\rangle$ it gives at leading order the length of the state L_2 . In conclusion, we have derived the following equality

$$|\langle \mathbf{1}^f | \tilde{\mathcal{O}}_3 |\mathbf{2}\rangle| = L_2 |\langle \mathbf{1}^f, \{\hat{p}_j^{(1)}\} | \tilde{\mathcal{O}}_3 |\mathbf{2}, \{\hat{p}_i^{(2)}\}\rangle|. \quad (\text{E.4})$$

The relation above shows how the structure constant changes under $\mathfrak{su}(1|1)$ transformations of the states $|\mathbf{2}\rangle$ and $\langle \mathbf{1}^f|$ at leading order. It is now simple to check that our expression for this scalar product given in the main text indeed satisfies this relation.

At one-loop, the final expression for the structure constants given in (3.10) has the following term

$$\langle \mathbf{1}^f | \tilde{\mathcal{O}}'_3 | \mathbf{2} \rangle, \quad (\text{E.5})$$

where

$$\tilde{\mathcal{O}}'_3 = \left(1 + \frac{g^2}{2} \mathcal{F}_{L_3-N_3, L_3-N_3+1} + \frac{g^2}{2} \mathcal{F}_{L_1,1} \right) \tilde{\mathcal{O}}_3 \left(1 + \frac{g^2}{2} \mathcal{F}_{N_3, N_3+1} + \frac{g^2}{2} \mathcal{F}_{L_2,1} \right). \quad (\text{E.6})$$

If we require that $\tilde{\mathcal{O}}'_3$ commutes with the generator $\tilde{\mathfrak{S}}$ then we find that at one-loop the relation (E.4) becomes

$$| \langle \mathbf{1}^f | \tilde{\mathcal{O}}'_3 | \mathbf{2} \rangle | = \left(L_2 + \frac{1}{2} \gamma_2 \right) | \langle \mathbf{1}^f, \{\hat{p}_j^{(1)}\} | \tilde{\mathcal{O}}'_3 | \mathbf{2}, \{\hat{p}_i^{(2)}\} \rangle |, \quad (\text{E.7})$$

where γ_2 is the one-loop anomalous dimension of the operator \mathcal{O}_2 . We have verified that this relation is indeed obeyed, which shows that our prescription respects these symmetry constraints.

References

- [1] N. Gromov, V. Kazakov and P. Vieira, “Exact Spectrum of Anomalous Dimensions of Planar N=4 Supersymmetric Yang-Mills Theory,” *Phys. Rev. Lett.* **103**, 131601 (2009) [arXiv:0901.3753 [hep-th]].
- [2] N. Beisert, C. Ahn, L. F. Alday, Z. Bajnok, J. M. Drummond, L. Freyhult, N. Gromov and R. A. Janik *et al.*, “Review of AdS/CFT Integrability: An Overview,” *Lett. Math. Phys.* **99**, 3 (2012) [arXiv:1012.3982 [hep-th]].
- [3] N. Gromov, V. Kazakov, S. Leurent and D. Volin, “Quantum spectral curve for AdS_5/CFT_4 ,” *Phys. Rev. Lett.* **112**, 011602 (2014) [arXiv:1305.1939 [hep-th]].
- [4] J. Escobedo, N. Gromov, A. Sever and P. Vieira, “Tailoring Three-Point Functions and Integrability,” *JHEP* **1109**, 028 (2011) [arXiv:1012.2475 [hep-th]].
- [5] O. Foda, “N=4 SYM structure constants as determinants,” *JHEP* **1203**, 096 (2012) [arXiv:1111.4663 [math-ph]].
- [6] K. Okuyama and L. -S. Tseng, “Three-point functions in N = 4 SYM theory at one-loop,” *JHEP* **0408**, 055 (2004) [hep-th/0404190].
- [7] L. F. Alday, J. R. David, E. Gava and K. S. Narain, “Structure constants of planar N = 4 Yang Mills at one loop,” *JHEP* **0509**, 070 (2005) [hep-th/0502186].

- [8] N. Gromov and P. Vieira, “Tailoring Three-Point Functions and Integrability IV. Theta-morphism,” arXiv:1205.5288 [hep-th].
- [9] Y. Jiang, I. Kostov, F. Loebbert and D. Serban, “Fixing the Quantum Three-Point Function,” arXiv:1401.0384 [hep-th].
- [10] P. Vieira and T. Wang, “Tailoring Non-Compact Spin Chains,” [hep-th/1311.6404].
- [11] V. Kazakov and E. Sobko, “Three-point correlators of twist-2 operators in N=4 SYM at Born approximation,” JHEP **1306**, 061 (2013) [arXiv:1212.6563 [hep-th]].
- [12] O. Foda, Y. Jiang, I. Kostov and D. Serban, “A tree-level 3-point function in the $su(3)$ -sector of planar $N = 4$ SYM,” arXiv:1302.3539 [hep-th].
- [13] M. Staudacher, “The Factorized S-matrix of CFT/AdS,” JHEP **0505**, 054 (2005) [hep-th/0412188].
- [14] G. M. Sotkov and R. P. Zaikov, “Conformal Invariant Two Point and Three Point Functions for Fields with Arbitrary Spin,” Rept. Math. Phys. **12**, 375 (1977).
- [15] G. M. Sotkov and R. P. Zaikov, “On the Structure of the Conformal Covariant N Point Functions,” Rept. Math. Phys. **19**, 335 (1984).
- [16] M. S. Costa, J. Penedones, D. Poland and S. Rychkov, “Spinning Conformal Correlators,” JHEP **1111**, 071 (2011) [arXiv:1107.3554 [hep-th]].
- [17] N. Beisert, “The $su(2+3)$ dynamic spin chain,” Nucl. Phys. B **682**, 487 (2004) [hep-th/0310252].
- [18] J. A. Minahan and K. Zarembo, “The Bethe ansatz for N=4 superYang-Mills,” JHEP **0303**, 013 (2003) [hep-th/0212208].
- [19] S. Lee, S. Minwalla, M. Rangamani and N. Seiberg, “Three point functions of chiral operators in $D = 4$, N=4 SYM at large N,” Adv. Theor. Math. Phys. **2**, 697 (1998) [hep-th/9806074].
- [20] M. Wheeler, “Scalar products in generalized models with $SU(3)$ -symmetry,” [arXiv:1204.2089 [math-ph]].
- [21] M. Wheeler, “Multiple integral formulae for the scalar product of on-shell and off-shell Bethe vectors in $SU(3)$ -invariant models,” Nucl. Phys. B **875**, 186 (2013) [arXiv:1306.0552 [math-ph]].
- [22] S. Pakuliak, E. Ragoucy and N. A. Slavnov, “Scalar products in models with $GL(3)$ trigonometric R-matrix. Highest coefficient,” [arXiv:1311.3500 [math-ph]].
- [23] S. Belliard, S. Pakuliak, E. Ragoucy and N. A. Slavnov, “Highest coefficient of scalar products in $SU(3)$ -invariant integrable models,” J. Stat. Mech. (2012) P09003, [arXiv:1206.4931 [math-ph]].

- [24] T. Klose and T. McLoughlin, “Worldsheet Form Factors in AdS/CFT,” *Phys. Rev. D* **87**, 026004 (2013) [arXiv:1208.2020 [hep-th]].
- [25] T. Klose and T. McLoughlin, “Comments on World-Sheet Form Factors in AdS/CFT,” arXiv:1307.3506.
- [26] B. Basso, A. Sever and P. Vieira, “Space-time S-matrix and Flux-tube S-matrix at Finite Coupling,” *Phys. Rev. Lett.* **111**, 091602 (2013) [arXiv:1303.1396 [hep-th]].
- [27] B. Basso, A. Sever and P. Vieira, “Space-time S-matrix and Flux tube S-matrix II. Extracting and Matching Data,” *JHEP* **1401**, 008 (2014) [arXiv:1306.2058 [hep-th]].
- [28] B. Basso, A. Sever and P. Vieira, “Space-time S-matrix and Flux-tube S-matrix III. The two-particle contributions,” arXiv:1402.3307 [hep-th].
- [29] G. Georgiou, V. L. Gili and R. Russo, “Operator Mixing and the AdS/CFT correspondence,” *JHEP* **0901** (2009) 082 [arXiv:0810.0499 [hep-th]].
- [30] G. Georgiou, V. Gili, A. Grossardt and J. Plefka, “Three-point functions in planar N=4 super Yang-Mills Theory for scalar operators up to length five at the one-loop order,” *JHEP* **1204**, 038 (2012) [arXiv:1201.0992 [hep-th]].
- [31] B. Eden, P. Heslop, G. P. Korchemsky and E. Sokatchev, *Nucl. Phys. B* **869** (2013) 329 [arXiv:1103.3714 [hep-th]].
- [32] N. Beisert, C. Kristjansen, J. Plefka, G. W. Semenoff and M. Staudacher, “BMN correlators and operator mixing in N=4 superYang-Mills theory,” *Nucl. Phys. B* **650**, 125 (2003) [hep-th/0208178].
- [33] G. Georgiou and G. Travaglini, “Fermion BMN operators, the dilatation operator of N=4 SYM, and pp wave string interactions,” *JHEP* **0404**, 001 (2004) [hep-th/0403188].
- [34] N. Beisert, “The Dilatation operator of N=4 super Yang-Mills theory and integrability,” *Phys. Rept.* **405**, 1 (2004) [hep-th/0407277].